DM

PyPort
A Modeling, Simulation and Optimization Platform for Maritime-Touristic Operations

MASTER DISSERTATION

Toni Jaime Abreu Garcês
MASTER IN INFORMATICS ENGINEERING

UNIVERSIDADE da MADEIRA
A Nossa Universidade
www.uma.pt

February | 2026

PyPort
A Modeling, Simulation and Optimization Platform for Maritime-Touristic Operations

MASTER DISSERTATION

Toni Jaime Abreu Garcês
MASTER IN INFORMATICS ENGINEERING

SUPERVISOR
Amâncio Lucas de Sousa Pereira

CO-SUPERVISOR
Filipe Magno de Gouveia Quintal

Faculdade de Ciências Exatas e da Engenharia

Master of Science Degree in Informatics Engineering

PyPort: A Modeling, Simulation and Optimization Platform for Maritime-Touristic Operations

Toni Jaime Abreu Garcês

Supervised by:

Dr. Amâncio Lucas de Sousa Pereira

Prof. Filipe Magno de Gouveia Quintal

Constituição do júri de provas públicas:

Prof. Karolina Baras, Presidente

Prof. Fábio Mendonça, Vogal

Dr. Lucas Pereira, Vogal

March, 2026

Resumo

O setor marítimo está a caminhar para a sustentabilidade, com esforços para reduzir as emissões, adotar embarcações elétricas e melhorar a gestão energética nos portos. Na área do turismo marítimo, especialmente nos portos de recreio, a eletrificação tem o potencial de provocar mudanças significativas. Esta transição afetará não só a forma como os portos utilizam eletricidade, mas poderá também exigir ajustes nas infraestruturas adjacentes e nos modelos de negócio. A eletrificação das operações portuárias pode ser mais desafiante devido à necessidade de sistemas de carregamento eficientes, tornando o planeamento essencial.

Um dos principais desafios neste domínio é a falta de dados reais que apoiem a investigação e a tomada de decisões. Para colmatar esta lacuna, esta tese centra-se na criação de um simulador concebido para portos de recreio. O simulador incluirá modelos de embarcações, de baterias, de rotas e de estratégias de carregamento, utilizando uma combinação de dados reais e cenários gerados.

O objetivo desta ferramenta é melhorar as operações portuárias, equilibrando as necessidades energéticas, reduzindo as emissões e promovendo a sustentabilidade. Ao fornecer uma forma de estudar estas questões, o simulador ajudará a ultrapassar os desafios atuais e a apoiar o desenvolvimento da eletrificação no setor do turismo marítimo.

Palavras-chave: setor marítimo, eletrificação de navios, digital twins, modelação de barcos, controlo de carregamento

Abstract

The maritime sector is moving toward sustainability with efforts to reduce emissions, adopt electric vessels, and improve port energy management. In the maritime-tourism area, particularly in recreational ports, electrification has the potential to bring about significant changes. This transition will not only affect how ports use electricity, but may also require adjustments to nearby infrastructure and business models. The electrification of port operations can be more challenging due to the need for efficient charging systems, making careful planning essential.

A major challenge in this field is the lack of real-world data to support research and decision making. To address this, this thesis focuses on creating a simulator designed for recreational ports. The simulator will include models of vessel propulsion, battery systems, routes, and charging strategies using a mixture of real-world data and generated scenarios.

The goal of this tool is to improve port operations by balancing energy needs, reducing emissions, and supporting sustainability. By providing a way to study these issues, the simulator will help overcome current challenges and support the development of electrification in the maritime tourism sector.

Keywords: maritime sector, vessel electrification, digital twins, vessel modeling, charging control

Acknowledgments

I would like to begin by expressing my sincere gratitude to my supervisor, Lucas Pereira, for his dedicated guidance, thoughtful feedback, and continuous support throughout the development of this thesis.

I am also deeply thankful to my family and friends for their unwavering encouragement, understanding, and patience. Their support provided me with the strength and motivation necessary to complete this important stage of my life.

Lastly, I sincerely acknowledge the opportunity to conduct this research within the AHEAD project, expressing my gratitude to all of its members for their collaboration and support, as well as to the University of Madeira for providing the academic environment and institutional conditions that made this achievement possible.

Table of Contents

List of Figures

List of Tables

List of Acronyms

AC Alternating Current

ADMM Alternating Direction Method of Multipliers

AI Artificial Intelligence

ANN Artificial Neural Networks

B2G Boat-to-Grid

BAP Berth Allocation Problem

BESS Battery Energy Storage System

BIM Building Information Modeling

BST Battery Swapping Technology

CCS Combined Charging System

DC Direct Current

DCNN Dilated Convolutional Neural Networks

DER Distributed Energy Resources

DHI Diffuse Horizontal Irradiance

DL Deep Learning

DNI Direct Normal Irradiance

DT Digital Twin

EAV Entity Attribute Value

EMS Energy Management System

ER Entity-Relationship

ETS Emissions Trading System

EU European Union

EV Electric Vehicle

EVSE Electric Vehicle Supply Equipment

GHG Greenhouse Gas

GHI Global Horizontal Irradiance

GPR Gaussian Process Regression

HMMs Hidden Markov Models

HVSC High-Voltage Shore Connection

IMO International Maritime Organization

IoT Internet of Things

KPI Key Performance Indicators

LSBoost Least-Squares Boosting

LSTM Long Short-Term Memory

LVSC Low-Voltage Shore Connection

MCS Megawatt Charging System

MILP Mixed-Integer Linear Program

ML Machine Learning

NASA National Aeronautics and Space Administration

NWP Numerical Weather Prediction

OOP Object-Oriented Programming

OPS Onshore Power Supply

PLM Product Life-Cycle Management

POA Plane-of-Array

PV Photovoltaic

RES Renewable Energy Sources

RF Random Forest

RLSTM Residual Long Short-Term Memory

SCIP Solving Constraint Integer Programs

SCR Self-Consumption Rate

SOC State of Charge

SSE Shore-Side Electricity

SSR Self-Sufficiency Rate

STC Standard Test Conditions

STS Shore-to-Ship

SUC System Use Case

TCO Total Cost of Operation

V2G Vehicle-to-Grid

WRF Weather Research and Forecasting

1 Introduction

The global push towards decarbonization has highlighted the urgent need for sustainable solutions across industries, with the maritime sector emerging as a crucial focus. As the International Maritime Organization (IMO) has committed to cutting total annual greenhouse-gas emissions from international shipping by at least 50% by 2050 compared to 2008 levels, electrification of marine vessels and ports is becoming a central strategy. [1]

Among the first innovations, lithium-ion battery systems enable hybrid and fully electric marine vessels. Cold ironing technology, which allows docked ships to draw power from shore grids instead of running auxiliary engines, further supports this initiative in port cities [2]. This technology, also known as Onshore Power Supply (OPS), has seen a significant push in various regions, including Europe, where efforts to implement it in all ports by 2025 were reported to be underway in 2021 [3]. However, due to significant challenges such as high costs and insufficient grid capacity, the timeline has been extended. Although some ports are on track, others are expected to require additional years, with deployment continuing until the 2030s in many locations [4].

In addition, recreational ports are progressively perceived as having a unique position in this transformation. Although they contribute significantly to local economies and social well-being, they also pose environmental challenges, such as pollution [5]. Sustainable marine development, by modernizing recreational ports with environmentally friendly infrastructure, including electrified berthing facilities and waste management systems, highlights the potential of recreational ports to align with global decarbonization goals [6].

This shift is also evident in other European initiatives like *SHIFT2DC*[1] and *AHEAD*[2], which aim to advance energy efficiency and sustainability in various sectors. *SHIFT2DC* focuses on integrating Direct Current (DC) solutions into infrastructures such as data centers, ports, buildings, and industries. The *AHEAD* project aims to develop a simulation environment to optimally place Electric Vehicle (EV) charging stations while efficiently utilizing the resources of the power grid in urban and rural areas. Besides EVs, the *AHEAD* project will also consider the challenges of charging vessels.

[1] https://shift2dc.eu
[2] https://horizon-ahead.eu

Developing models for recreational vessels and optimizing their operation is essential for maritime decarbonization. However, limited data on boating activities and energy use complicate the creation of effective solutions. This thesis delves into these areas, focusing primarily on modeling recreational boats and developing optimization control mechanisms for their charging processes. The project is carried out mainly within the scope of the *AHEAD* initiative, with insights from *SHIFT2DC*.

1.1 Context

As stated, this thesis is developed within the scope of two European initiatives: the *SHIFT2DC* and *AHEAD* projects, both of aim to advance energy management and sustainable mobility solutions by integrating renewable energy sources, innovative infrastructure, and digital tools.

The *SHIFT2DC* project is dedicated to promoting the adoption of medium and low voltage DC systems, which are designed to enhance energy efficiency and reduce carbon emissions in diverse applications including buildings, industries, and ports. The project aims to develop and test DC solutions that are scalable, interoperable, focusing on hybrid Alternating Current (AC)/DC systems. By conducting field tests and deploying demonstrators, *SHIFT2DC* evaluates the technical feasibility, life cycle costs, and environmental benefits of DC technologies, therefore fostering their broader adoption.

A central element of the *SHIFT2DC* initiative is the Port Demonstrator in Madeira Island, located at Funchal Port. This demonstrator addresses the unique energy challenges faced by ports, such as high power demands and the need for renewable energy integration, while also aligning with the environmental objectives set by the IMO. The demonstrator will feature renewable energy installations, including solar panels, battery storage systems, and hybrid AC/DC infrastructure. This thesis contributes to these efforts by developing a highly configurable simulation environment for the port's maritime-tourism area. Rather than a fully deployed Digital Twin (DT) fed by real-time sensor data, this simulator acts as a foundational precursor, facilitating scenario-based testing of future infrastructure and exploring innovative solutions such as microgrids and DC charging systems.

Complementing *SHIFT2DC*, the *AHEAD* project focuses on the integration of electric mobility systems into energy grids, utilizing tools Artificial Intelligence (AI) for planning and optimization. *AHEAD* targets the development of flexible charging infrastructure for vehicles and vessels. In

Funchal, the project also entails the maritime-tourism segment, integrating smaller vessels and urban charging solutions.

The synergy between these two initiatives creates the basis for transforming ports and surrounding areas into sustainable and energy efficient systems. More precisely, in the context of Funchal Port, the *SHIFT2DC* demonstrator exemplifies the potential of DC systems to address energy challenges while the *AHEAD* project contributes advanced tools and methodologies to enhance performance. With these efforts, the projects mean to establish Funchal Port as an example of low-carbon maritime innovation.

1.2 Objectives

The main objective of this thesis is to develop a simulation framework that acts as a vital precursor to a full Digital Twin, assessing the impact and benefits of electrifying recreational ports. The work places particular emphasis on modeling electric recreational vessels and their interaction with the port infrastructures, allowing the exploration of different charging strategies, energy flows, and integration of renewable energy sources. This simulator intends to contribute to the broader transition toward low-carbon maritime environments by providing a reliable planning tool.

To achieve this, the following goals are defined:

- Implement a modular simulation environment capable of evaluating port-wide electrification scenarios, including vessel charging, power generation, and storage components.
- Analyze the performance of different charging and energy management strategies with respect to cost, reliability, and grid constraints.
- Assess the potential contribution of renewable energy systems in supporting an electrified recreational port.

1.3 Research Questions

Motivated by the objectives outlined above and the need to bridge the gap between theoretical modeling and fully operational smart ports, this thesis addresses the following primary research question:

- *Can the dynamic operations of a fully electric recreational port be reliably simulated to assess the techno-economic impacts of its electrification?*

To further guide the development and evaluation of the proposed solution, the following question is also explored:

- *What are the tangible impacts of implementing optimization strategies on port operational reliability and grid utilization?*

1.4 Document Structure

This document is organized into seven chapters. Chapter 1 introduces the context, motivation, research questions, and objectives of the thesis, outlining the relevance of port electrification and the role of recreational vessels within this transition.

Chapter 2 presents the State of the Art, covering the fundamental concepts required for this work. These include Digital Twins, modeling approaches, forecasting techniques, and optimization methods. The chapter also highlights the existing research gap that motivates the development of the proposed simulator.

Chapter 3 generally describes the proposed solution and how each module works.

Chapter 4 describes the development of the simulator. It details the system requirements, overall architecture, and database structure. The modeling of each key component, such as recreational vessels, recreational trips, charging infrastructure, photovoltaic generation, and battery storage, is explained, along with the additional prediction and optimization modules. The chapter concludes with an overview of the simulation engine.

Chapter 5 outlines the methodology used to evaluate the simulator. It discusses the testing of individual modules, the definition of use cases and simulation scenarios, and the assessment of optimization strategies.

Chapter 6 presents the results obtained through the simulation environment. It interprets the outcomes and discusses how they address the research questions and objectives formulated in this introductory chapter.

Finally, Chapter 7 concludes the thesis by summarizing the main findings and their implications. It also identifies possible directions for future work based on the limitations and insights uncovered throughout the project.

2 State Of The Art

2.1 Digital Twins

The concept of the DT has emerged as a pivotal technology in the Industry 4.0 revolution, acting as a bridge between the physical and virtual worlds. While the terminology is relatively modern, the conceptual roots can be traced back to the 1960s and 1970s with National Aeronautics and Space Administration (NASA). During the Apollo 13 mission, NASA employed ground-based high-fidelity "mirrored systems" to replicate the spacecraft's condition and test corrective actions, a practice commonly regarded as a precursor to modern DT [7, 8].

However, the formal concept of the DT was introduced by Michael Grieves in 2002 within the context of Product Life-Cycle Management (PLM). Grieves proposed a model consisting of three primary elements: a physical product in real space, a virtual product in virtual space, and a connection of data and information flow that ties the two together [8, 9]. Since then, the definition has evolved to encompass the entire life-cycle of an asset. Modern definitions describe a DT as a virtual representation of an object or system that spans its life-cycle, updated from real-time data, and uses simulation, machine learning, and reasoning to help decision-making [9, 10].

2.1.1 Classification and Characteristics

A critical distinction in the literature, often identified as a common misconception, is the difference between a Digital Model, a Digital Shadow, and a Digital Twin. This distinction is primarily defined by the level of data integration and the direction of data flow [8, 9]. As illustrated in Figure 1:

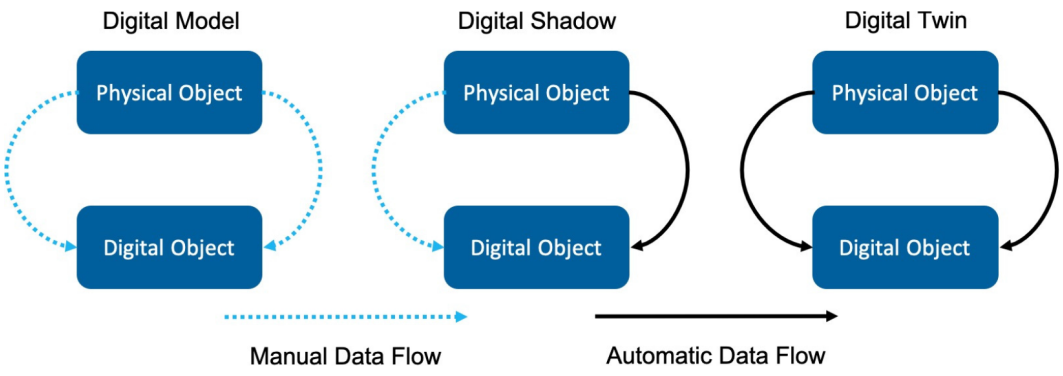

Figure. 1: Digital Model, Shadow, and Twin. Source: [9].

- **Digital Model:** A digital representation of a physical object where there is no automatic data exchange. Changes in the physical object do not automatically impact the digital version, and vice versa.
- **Digital Shadow:** A digital representation where there is a one-way automatic data flow from the physical object to the digital object. A change in the physical state leads to a change in the digital object, but not the other way around.
- **Digital Twin:** A fully integrated system where data flows automatically in both directions. A change in the physical object affects the digital object, and changes in the digital object can influence or control the physical object [9].

For a system to be considered a true DT, it requires specific characteristics: high-fidelity modeling, a seamless connection for real-time data exchange (often facilitated by the Internet of Things (IoT)), and the capability to perform data analytics for prediction and optimization [8]. However, recent literature argues that "fidelity" should not be confused with "complexity". A DT does not need to be an exact atomic replica of the physical object; rather, it requires sufficient accuracy to meet the specific simulation requirements of the user [11]. Furthermore, DTs can be categorized by scale, ranging from the component level to the asset level and finally the system level [12].

2.1.2 Enabling Technologies

The realization of DTs relies on a convergence of enabling technologies. The IoT and Industrial IoT (IIoT) serve as the sensory apparatus, collecting vast amounts of real-time data from the physical environment [9]. This data is processed using Big Data analytics and AI techniques, including machine learning and deep learning, to simulate behaviors and predict future states [13]. Additionally, spatial data capture technologies are increasingly used to create dimensionally accurate 3D digital replicas of built environments, providing the spatial context necessary for facility management [14].

In the context of Industry 5.0, the focus is shifting towards resilient and sustainable approaches. Here, DTs are not just tools for automation but facilitate human-machine collaboration [12]. This evolution is particularly relevant for complex systems where decision-making involves multiple stakeholders and environmental constraints.

2.1.3 Digital Twins in the Maritime Sector

While the aviation and manufacturing industries were early adopters of DT technology, the maritime sector has seen an exponential increase in DT research in recent years [15]. In this domain, DTs are applied across various life-cycle phases: design, manufacturing, operation, and maintenance. However, current research is predominantly focused on the operation phase, utilizing DTs for route planning, condition monitoring, and performance assessment [15].

Specifically, regarding port infrastructure, the DT is increasingly viewed as a "system of systems". Ports function as intersections between smart cities and global supply chains [16]. A holistic port DT requires three core capabilities:

1. **Situational Awareness:** Achieved through the virtual mirroring of all port processes.
2. **Intelligent Decision Making:** Utilizing comprehensive data analytics to optimize operations.
3. **Collaboration Interface:** Promoting multi-stakeholder governance, similar to Urban Digital Twins used in smart cities [16].

Recent frameworks for port DTs have begun to integrate Building Information Modeling (BIM) to address sustainability specifically. For instance, [17] developed an integrated DT for dry bulk terminals that combines cargo handling operations with building energy simulations. This approach allows for a granular assessment of energy consumption and emissions, not just from vessels, but from port facilities and buildings as well [17].

Despite these advancements, most maritime DT applications focus on commercial shipping logistics, container terminals, or specific vessel components [13, 15]. There is a significant emphasis on energy efficiency, with DTs being proposed to optimize the use of port facilities and equipment to reduce energy consumption and CO2 emissions [16]. However, literature dealing specifically with the electrification of recreational ports remains limited.

2.2 Electrification of Ports and Recreational Marinas

The electrification of the maritime-terrestrial interface is recognized as the foundation of the global strategy to decarbonize the shipping industry [18]. Although not directly representing recreational ports, as illustrated in Figure 2, the shipping sector (comprising both international and

domestic shipping) accounts for a notable percentage of global transportation emissions, underscoring the urgency of mitigation efforts.

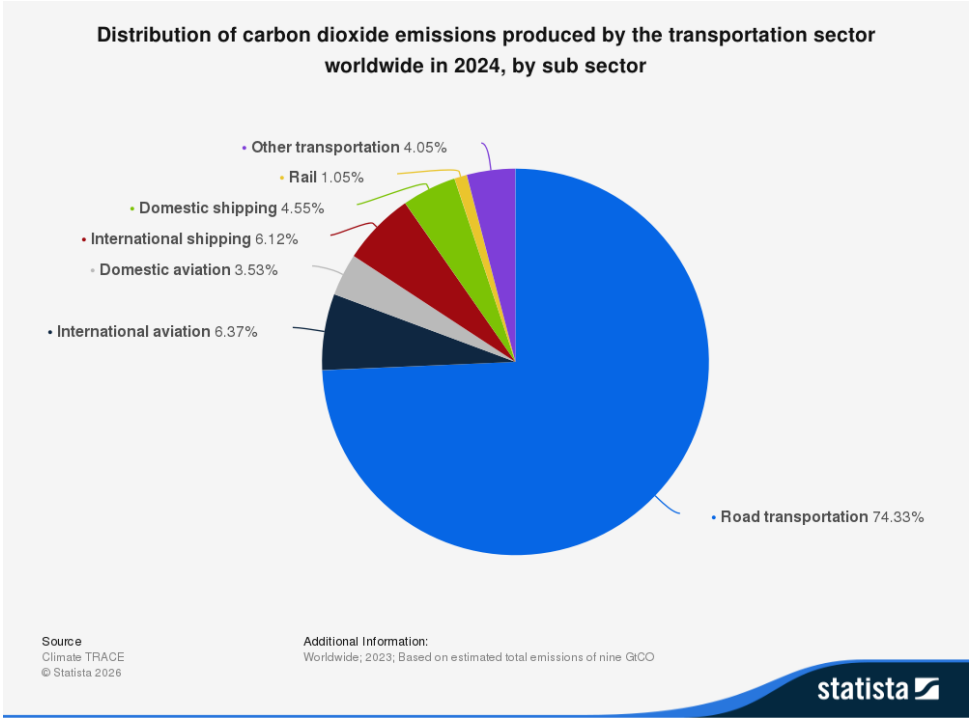

Figure. 2: CO2 Emissions by Transportation Sector 2023. Source: [19]

This transition is further driven by increasingly stringent environmental regulations, notably the IMO 2023 Greenhouse Gas Strategy, which aims for net-zero emissions by or around 2050 [20,21]. In the European context, the "Fit for 55" legislative package and the inclusion of maritime transport in the European Union (EU) Emissions Trading System (ETS) have accelerated the mandate for ports to provide electrical infrastructure, effectively internalizing the environmental costs of fossil fuel combustion at berth [22, 23].

2.2.1 Port Electrification and Shore Power Systems

Central to port electrification is the implementation of OPS, also widely referred to as cold ironing, Shore-Side Electricity (SSE), or Shore-to-Ship (STS) power supply [24, 25]. These systems enable vessels to shut down their auxiliary diesel engines while docked, drawing power from the land-based grid to maintain essential "hotel" functions such as lighting, climate control, and cargo handling [18, 22]. The adoption of OPS can reduce local and particulate matter emissions by over

90%, while the reduction in overall Greenhouse Gas (GHG) depends heavily on the carbon intensity of the local electrical grid [18, 21].

Technical implementation of OPS involves a complex chain consisting of the shore-side substation, a cable management system for the ship-to-shore interface, and the onboard receiving equipment [24, 26]. A primary technical barrier is the lack of uniformity in electrical parameters; approximately 75% of the global fleet operates at 60 Hz, whereas many terrestrial grids, particularly in Europe, operate at 50 Hz [18]. This necessitates the use of large-scale frequency converters and transformers to bridge the gap between High-Voltage Shore Connection (HVSC) and Low-Voltage Shore Connection (LVSC) requirements [18, 27]. To facilitate global interoperability, the industry relies on the ISO/IEC/IEEE 80005 series of standards, which define the requirements for high-voltage connections, data communication protocols for monitoring and control, and low-voltage systems [18, 27]. Despite these standards, high capital expenditures create a deadlock where ports hesitate to invest without guaranteed outcomes or demand by shipowners, challenging widespread deployment [24, 26].

2.2.2 Electrification of Recreational and Small Electric Vessels

While large commercial ports focus on industrial OPS, recreational marinas and small-scale ports are undergoing a transition toward becoming "Smart Energy Hubs" [23]. This segment of the maritime fleet, which includes all-electric ferries, tugboats, and recreational pleasure craft, often utilizes high-capacity battery systems that require frequent charging during short port stays [24,27].

The electrification of these smaller vessels is increasingly integrated into the broader Industry 4.0 and Smart Port paradigms [28]. Frameworks such as the Proteus plan advocate for a holistic energy management approach where marinas incorporate Renewable Energy Sources (RES), such as solar and wind, coupled with Battery Energy Storage System (BESS) to manage peak demand and stabilize the local microgrid [23].

Innovative charging strategies are being explored to overcome the limitations of traditional cable connections. These include Battery Swapping Technology (BST), which reduces downtime for commercial vessels, and the adaptation of terrestrial charging standards like the Combined Charging System (CCS) and Megawatt Charging System (MCS) for maritime use [24, 27]. Furthermore, the concept of "reverse cold ironing" or Vehicle-to-Grid (V2G) applications in the maritime

sector is gaining attention. On this topic, berthed vessels with large battery capacities can act as distributed energy resources, providing grid services or emergency power back to the port infrastructure during periods of high demand [23]. As these technologies mature, the focus is shifting from simple power supply to an integrated, bidirectional energy ecosystem that enhances both the sustainability and resilience of recreational maritime facilities [23, 28].

2.3 System Modeling for Electrified Recreational Ports

The transition toward electrified maritime facilities necessitates a multi-domain modeling approach that captures the interactions between mobile loads, charging interfaces, and the terrestrial grid. Unlike traditional port infrastructures, electrified recreational marinas act as complex energy hubs where the irregular nature of vessel arrivals and the variable energy demands of electric propulsion systems must be harmonized with localized generation and storage. A comprehensive system model is therefore required to ensure operational reliability, optimize energy costs, and assess the impact of high-power charging on the local microgrid stability. This subsection reviews the modeling techniques for the three core components of this ecosystem: the electric vessel, the charging station, and the port energy infrastructure.

2.3.1 Electric Vessel Energy Consumption Modeling

Accurate energy consumption modeling is fundamental for determining the battery requirements and operational autonomy of electric vessels. The primary determinant of energy demand in maritime propulsion is the relationship between ship speed and the power required. As discussed by [29], this is traditionally governed by the propeller law, also known as the "cube law", which states that the power required to propel a vessel is proportional to the cube of its speed:

$$P(v) = k \cdot v^3 \tag{1}$$

where k is a vessel-specific constant representing hydrodynamic efficiency and hull characteristics. While this law serves as a theoretical baseline, [29] argues that regression analyses of real-world data often reveal exponents that vary depending on ship type and operational conditions, warning against the pitfalls of simplified models in policy-making.

Furthermore, the marine environment introduces random loads that must be accounted for in high-fidelity models. [30] proposes a predictive modeling approach for electric propulsion ships

that incorporates environmental loads such as wind, waves, and currents, noting that these factors significantly alter the torque requirements of the propulsion motor. For the specific case of small-scale maritime transport, [31] emphasizes the importance of voyage cycle modeling, utilizing GPS data and route characteristics to estimate the State of Charge (SOC) depletion and define the necessary battery capacity for electrification.

2.3.2 Charging Infrastructure Modeling

Modeling the charging interface is critical for assessing the impact of electrified vessels on the port's electrical grid. Maritime charging involves high-power demands that must adhere to emerging international standards. [32] highlights that technical modeling of shore-side charging must consider the standard requirements for connectors and communication protocols, such as the ISO/IEC 80005 series, to ensure interoperability between diverse vessel types and shore-power systems.

The load profile of a charging station can be modeled using processes to account for the arrival times and initial SOC of arriving vessels. [33] suggests that modeling charging station loads requires a consideration of different charging technologies and their respective efficiency curves, characterizing the peak demand on the distribution network.

2.3.3 Port Energy Infrastructure and Microgrid Modeling

To support the transition to electric mobility, recreational ports are being modeled as complex microgrids that integrate RES, BESS, and OPS. [34] provides a framework for designing harbor grid models, analyzing different configurations to facilitate both the charging of onboard batteries and the supply of shore power to berthed vessels across multiple operational scenarios.

The integration of sustainable energy is often modeled through multi-level optimization frameworks. [35] demonstrates capacity planning for port microgrids under carbon constraints, focusing on the optimal sizing of Photovoltaic (PV) and BESS components to minimize life-cycle costs using bi-level cost optimization. For stability and resilience analysis, [36] employs intelligent modeling of PV-BESS microgrids in MATLAB/Simulink to evaluate the system's resilience and prevent blackouts during peak demand or system disturbances. Similarly, [37] models isolated microgrids with a specific focus on peak load shaving, illustrating how the BESS can be dispatched to mitigate the impact of vessel charging on the local grid. Finally, [38] emphasizes the necessity of comprehensive

power flow modeling and analysis to ensure that green seaport power systems maintain voltage stability and reliability under varying operational conditions.

2.4 Forecasting in Port Energy Systems

The effective management of an electrified port microgrid relies heavily on the ability to anticipate both the availability of intermittent renewable resources and the highly variable load demands of port operations [39, 40]. Thus, port energy systems are characterized by heavy loads that are strongly correlated with logistic activities [41]. Consequently, accurate forecasting has become a prerequisite for optimization tasks such as peak shaving, energy arbitrage, and infrastructure planning [42, 43].

2.4.1 Renewable Energy Generation Forecasting

The integration of RES, particularly PV and wind power, introduces significant uncertainty into the port energy mix due to their dependence on meteorological conditions [44]. Forecasting methodologies for these resources are generally categorized into physical models, statistical models, and machine learning approaches [44].

Physical models rely on Numerical Weather Prediction (NWP) data to simulate the output of energy systems. For instance, [40] utilized the Weather Research and Forecasting (WRF) model to estimate the solar and wind potential for a cold ironing system in the Port of Ancona. In this approach, the power output of wind turbines is calculated as a function of air density, rotor area, and wind speed cubed, while PV output is derived from incident solar radiation and cell temperature, adjusted by a derating factor [40].

However, traditional physical and shallow statistical models often struggle with the non-linear and volatile nature of solar irradiance in short-term horizons [44]. To address this, hybrid Deep Learning (DL) architectures have been proposed. [44] developed a hybrid network combining Dilated Convolutional Neural Networks (DCNN) to extract spatial features from historical weather data, and Residual Long Short-Term Memory (RLSTM) networks to capture temporal correlations. This "end-to-end" learning capability allows for more precise forecasting compared to standalone models [44].

Furthermore, recent research emphasizes that forecasting should not be an isolated task but coupled with downstream decision-making. [39] proposed a decision-focused framework where a probabilistic forecasting model is jointly optimized with a robust operation model. By minimizing "decision regret" rather than just statistical error, the forecast directly enhances the economic efficiency and robustness of the microgrid schedule [39].

2.4.2 Energy Demand Forecasting in Ports and Marinas

Forecasting electricity demand in ports is distinct from standard residential or commercial load forecasting due to the "event-driven" nature of maritime logistics [41, 45]. The irregular arrival of vessels with the simultaneous port operations can cause abrupt load spikes that purely historical time-series models fail to predict [42]. Literature typically classifies approaches into simulation-based and data-driven methods [42].

Due to the scarcity of high-quality historical meter data in many ports, simulation-based approaches are often employed to construct the total load profile by aggregating the estimated consumption of individual assets [42]. Specifically towards container ports, [41] argues that traditional data-driven models are unsuitable because the load exhibits weak inherent regularity but strong correlation with the ship arrival and departure schedules. They proposed a method that calculates the power profile based on the specific operational steps of quay cranes and the volume of containers to be handled per vessel [41]. Similarly, [40] reconstructed the load profile of the Port of Ancona by analyzing the specific power requirements and berthing durations of ferry traffic to dimension an OPS system.

With the increasing deployment of smart metering, data-driven techniques are gaining traction. [46] categorizes these into very short-term (minutes), short-term (hours to weeks), and long-term (years) horizons, noting that new environments like smart grids require adaptive techniques capable of integrating demand, generation, and storage. For long-term planning, [43] applied an Long Short-Term Memory (LSTM) model trained on 10 years of data to forecast the power consumption of Busan New Port, identifying a strong correlation between container throughput and electricity usage. Their results highlighted that power consumption is growing faster than throughput due to the increasing automation and electrification of port equipment [43].

For short-term operational forecasting, advanced Machine Learning (ML) models are required to handle volatility. [45] developed a comparative framework for port microgrids, evaluating Random Forest (RF), Least-Squares Boosting (LSBoost), and Gaussian Process Regression (GPR). They found that RF provided the highest accuracy for 24-hour ahead forecasts. Crucially, their study demonstrated that incorporating "Weighted Port Calls", a feature combining ship count with vessel technical parameters, significantly improved model performance compared to using historical load data alone [45].

To address extreme volatility, [47] introduced a new LSTM model enhanced by a Dual-Attention mechanism. This architecture dynamically filters input noise and captures both fine-grained short-term fluctuations and long-term dependencies, outperforming traditional baselines in complex port environments [47]. Additionally, regarding the integration of electric vehicles and dynamic changes in consumption patterns, [48] proposed an adaptive online learning method using Hidden Markov Models (HMMs). This approach recursively updates model parameters to adapt to new data, a feature essential for recreational ports undergoing electrification and infrastructure changes [48].

2.5 Optimization and Energy Management Strategies

The transition to smart ports necessitates advanced control strategies that go beyond simple load monitoring. Recent literature emphasizes the deployment of Energy Management System (EMS) to coordinate the RES, the rigid constraints of maritime logistics, and the flexibility of storage systems. [49] demonstrates that implementing an EMS in smart ports can reduce annual energy consumption by approximately 7-8% and carbon emissions by 11-12%, while achieving operational cost savings of up to 30%.

2.5.1 Energy Management of Microgrids

Optimization in port microgrids is typically addressed through centralized or distributed mathematical frameworks aimed at minimizing life-cycle costs and environmental impacts. A common approach involves Mixed-Integer Linear Program (MILP) due to its ability to handle logical constraints and guarantee global optimality. [50] developed a MILP-based methodology for the simultaneous optimization of microgrid sizing and energy management in the port of Martinique. Their model incorporates economic and environmental criteria to manage PV generation and storage, ensuring that OPS demands are met while minimizing the cost of energy [50].

As energy systems become more complex, hierarchical and bi-level optimization frameworks are gaining prominence. [51] proposed a hierarchical multi-objective co-optimization framework for a Port that couples hydrogen and electricity. In this structure, the upper level optimizes the capacity configuration of equipment to minimize annual investment costs, while the lower level optimizes the hourly energy management to minimize operating costs and carbon emissions [51].

Furthermore, to address the privacy concerns and computational burdens of centralized controllers, distributed optimization methods are being explored. [52] introduced a distributed energy scheduling method using the Alternating Direction Method of Multipliers (ADMM). This approach allows different stakeholders within the port to optimize their local objectives individually while coordinating through information exchange, effectively integrating energy generation with flexible port loads [52]. Additionally, hybrid approaches combining optimization with ML are emerging; [53] utilized Artificial Neural Networks (ANN) to predict energy efficiency indicators, which were then fed into heuristic optimization algorithms to balance hybrid energy sources including wind, solar, and water.

2.5.2 Optimization in Electrified Maritime and Marina Systems

A distinguishing feature of maritime optimization is the strong coupling between ship operations and energy consumption. [54] addressed this by integrating operations planning with energy management, using a MILP model optimize the microgrid power dispatch. Their findings indicate that shifting operations to times of high renewable availability or low electricity prices can significantly reduce peak power demand [54].

Similarly, [55] proposed a two-level optimization framework for seaside operations. The first level handles the Berth Allocation Problem (BAP) to minimize vessel service time, while the second level manages the microgrid energy flow and cold ironing assignment. This approach ensures that the energy supply strategy adapts to the physical movement of vessels, prioritizing green energy usage for cold ironing to mitigate emissions [55]. On the vessel side, optimization strategies are being applied to hybrid propulsion systems to minimize fuel consumption and emissions during operation, which in turn dictates the charging requirements upon berthing [56].

In the specific context of recreational marinas, the focus shifts from cargo efficiency to the flexibility of leisure boats. [57] investigated the potential of using electric boats as flexible loads

within a marina energy system. By modeling boats as deferrable loads, they demonstrated that optimizing the charging start times based on PV availability and grid prices could reduce the marina's net present cost and improve the self-consumption of locally generated energy [57].

Building on this, [58] explored the concept of Boat-to-Grid (B2G) for revenue generation in marinas. Their optimization model evaluated various revenue streams, including peak shaving and arbitrage on the spot market. The study concluded that utilizing the aggregate battery capacity of electric leisure boats for grid services could generate significant economic value, transforming the marina from a simple consumer into an active grid participant [58].

2.6 Research Gap

Despite the significant advancements in maritime electrification and microgrid optimization reviewed in this chapter, a critical analysis of the current literature reveals two distinct gaps, particularly concerning the recreational maritime sector.

1. Scarcity of Research on Recreational Marinas as Energy Hubs: The vast majority of existing research on port DTs, OPS, and energy management focuses predominantly on large-scale commercial ports, container terminals, and industrial shipping logistics. While the "Smart Port" concept is well-defined for these entities, the recreational marina sector remains underrepresented. Recreational marinas exhibit distinct operational characteristics, such as high seasonality, stochastic vessel arrival patterns, and longer berthing durations, that differ fundamentally from cargo ports.

2. Lack of Configurable Tools as DT Precursors: While the concept of the DT is gaining traction, most applications focus on the operation phase using real-time data streams, which implies a high entry barrier regarding sensor infrastructure and cost. There is a significant gap in the planning and design phase, specifically, the need for a "precursor" to a DT. Stakeholders lack flexible, scenario-based simulation environments that allow for the configuration of assets to test "what-if" scenarios before implementation. A tool that serves as a holistic simulator to assess the techno-economic impacts of electrification strategies and facilitate informed decision-making is currently missing.

This thesis aims to bridge these gaps by developing a holistic, multi-domain simulator for recreational marinas, providing a foundational layer for a future recreational marina DT.

3 Proposed Solution

This chapter introduces *PyPort Sim*, the simulation framework developed to address the challenges of electrifying recreational ports. As identified in the previous chapters, the lack of data and the unpredictable nature of recreational boating demand require a flexible, modular tool capable of assessing different scenarios. *PyPort Sim* is designed as a modular simulator that functions as a digital representation of the port's energy ecosystem. The proposed solution is built on a modular architecture, enabling the independent development and testing of key components, including vessels, chargers, renewable energy sources, and energy management strategies. This methodology certifies that the tool is adaptable to different port sizes and configurations.

3.1 System Requirements

The development of this framework is guided by specific requirements to ensure the simulation accurately reflects the dynamics of an electric port microgrid. These are categorized into functional and non-functional requirements.

3.1.1 Functional Requirements

Functional requirements define the specific behaviors and functions the system must execute.

Simulation Execution: The system must perform discrete-time simulations with a configurable timestep. It shall support both batch execution, where the entire simulation horizon is executed as fast as possible, and real-time execution, where each simulation step is synchronized in real-time to enable hardware-in-the-loop testing, live data ingestion, or interactive monitoring.

Data Ingestion: The system must ingest static configuration data and route definitions, as well as environmental data from external APIs. All input data shall be persisted to ensure that simulations can be repeated multiple times under identical conditions, enabling fair comparison across scenarios and control strategies.

Operational Scheduling: The system must implement an operational scheduling mechanism that assigns trips to vessels based on scenario-specific inputs throughout the simulation to emulate real-world recreational port operations.

Energy Management: The engine must orchestrate power flows between PV generation, BESS, grid connection, and charging loads.

Data Logging: All simulation metrics must be persisted to a database at every timestep for post-simulation analysis.

Port Configuration: The system must support the definition of multiple port configurations through external configuration files, allowing users to specify port topology, available assets, and operational constraints without modifying the simulation code.

3.1.2 Non-Functional Requirements

Non-functional requirements describe system attributes such as performance, reliability, and maintainability.

Modularity: The architecture must be decoupled to allow independent updates or replacements of algorithms without affecting the core loop.

Extensibility: The system must support the addition of new assets without requiring internal simulation logic modifications.

Robustness: The simulation must handle operational anomalies gracefully, such as postponing trips if energy is insufficient or reverting to rule-based control if the optimizer fails to return a solution.

Reproducibility: Given the same initial seed and configuration files, the simulation must produce identical results to ensure valid comparative analysis of control strategies.

3.2 General Architecture

The architecture of *PyPort Sim* is defined by a data-centric design pattern that strictly decouples computation from state management. To satisfy the **Modularity** and **Reproducibility** requirements outlined in Section 3.1, the system is organized around a central persistence layer.

As illustrated in Figure 3, the framework comprises three high-level independent blocks, **Data Sources**, **Simulation Core**, and **Front-End**, which interact exclusively through a central **Storage Module**. This topology ensures that the *Simulation Core* remains stateless between executions, relying on the Storage Module to persist the system state in the underlying **PyPort DB**. The different components are described next.

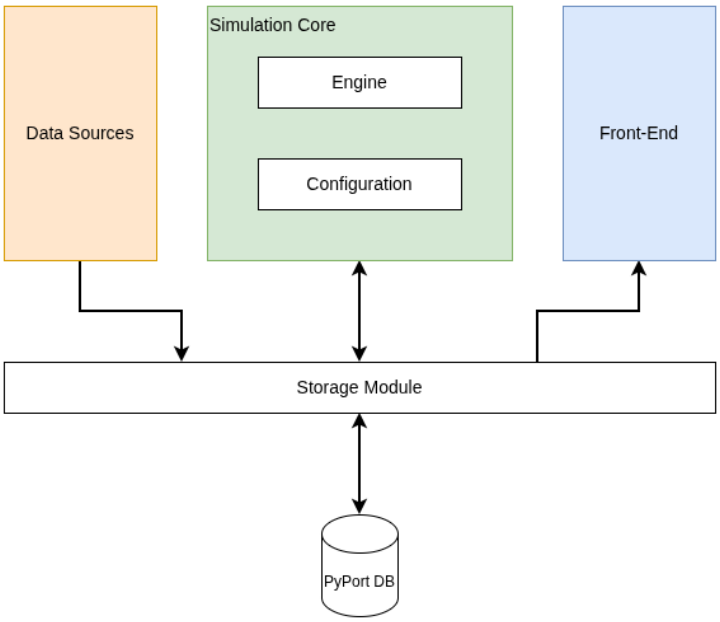

Figure. 3: High-level architecture of PyPort Sim.

3.2.1 Data Sources

The **Data Sources** block represents the ingestion layer of the framework. As illustrated in Figure 4, this module is responsible for collecting heterogeneous inputs from multiple origins.

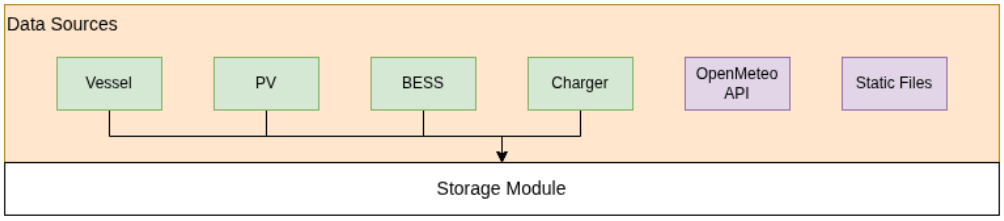

Figure. 4: Data sources and ingestion structure.

The inputs handled by this module are grouped into the following categories:

- **Component Models:** Parametric definitions of system components, including *Vessels*, *PV*, *BESS*, and *Chargers*. These models describe the technical specifications, operational limits, and performance characteristics of each device, and serve as the foundation for system behavior during the simulation.
- **OpenMeteo API:** An external interface used to retrieve environmental and meteorological data, such as solar irradiance and temperature. This information is primarily employed to generate renewable energy production profiles.

– **Static Files:** Configuration files that define fixed inputs required to execute the simulation. These include, but are not limited to, port electricity tariffs, predefined recreational vessel routes, which will be discussed in a later section, and fixed weather datasets for testing purposes.

3.2.2 Simulation Core

The **Simulation Core** encapsulates the computational logic of the simulator. As depicted in Figure 5, it is organized as a stack of modules, each responsible for a distinct aspect of the simulation. Some of these modules interact directly with the persistent Storage Module, while others operate independently of it.

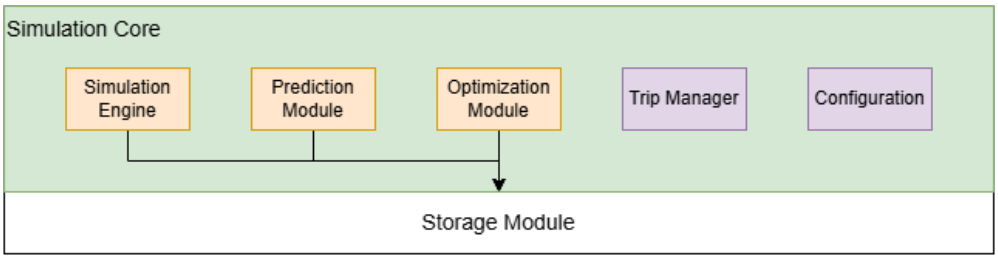

Figure. 5: Internal structure of the Simulation Core.

The core is composed of five sub-modules:

– **Simulation Engine:** The central orchestrator of the framework. It manages the discrete time-stepping mechanism of the simulation and coordinates the execution of the remaining modules. At each time step, it retrieves the current system state and updates the state after computation.

– **Prediction Module:** Responsible for generating look-ahead data for renewable energy production and load demand. These predictions are stored and retrieved through the Storage Module, as they are required by the Optimization Module in order to enable predictive control strategies.

– **Optimization Module:** Implements the energy management and control algorithms. Using the current system state and predicted information obtained from the Storage Module, it computes optimal power set-points and operational decisions for port assets such as PV Systems, BESS, and chargers. The resulting control actions are then written back to storage for execution and logging.

– **Trip Manager:** Handles the **Operational Scheduling** requirements of the system by dynamically assigning routes to vessels and updating their availability and operational status.

– **Configuration:** Implemented as the primary initialization script (`main.py`), it defines the port topology, instantiates system components, and configures simulation parameters. As its role is limited to setup and initialization, it does not rely on the Storage Module during runtime.

It is important to reinforce that *only* the *Simulation Engine*, *Prediction Module*, and *Optimization Module* maintain a direct connection to the Storage Module, as they require persistent access to historical states, predictions, and control decisions.

3.2.3 Front-End and Visualization

The **Front-End** represents the presentation and visualization layer of the framework. As illustrated in Figure 6, it is composed of a Dashboard that retrieves simulation outputs directly from the Storage Module.

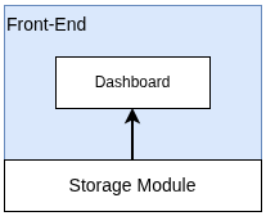

Figure. 6: Front-End visualization layer.

The Dashboard allows users to explore simulation results and evaluate Key Performance Indicators (KPI) through an interactive interface. By decoupling visualization from the Simulation Core, results can be analyzed without re-running the simulation, supporting the **Data Logging** requirement.

4 System Development

This chapter details the practical implementation of the system defined in the previous chapter. It transitions from the high-level architectural design to the concrete models, software structures, and algorithmic strategies employed to simulate the operation of an electric recreational port.

4.1 Implementation

This section describes the software implementation of the proposed framework, focusing on the modular organization of the codebase and the mechanisms used to persist simulation data and system states.

4.1.1 Project Structure

The implementation of *PyPort Sim* follows an Object-Oriented Programming (OOP) paradigm, where system components are modeled as interacting objects with specific responsibilities and interfaces. The codebase is organized into domain-specific packages, each encapsulating a distinct aspect of the simulation. The overall project organization is illustrated in Listing 1. The root directory contains the main entry points for the simulation (`main.py`) and the visualization dashboard (`streamlit_app.py`). The core functionality is distributed across sub-directories as follows:

- `models/`: Contains the class definitions representing the physical entities of the port, including vessels, generation units, and storage systems. These classes encapsulate both the internal state and the operational constraints of each asset, as detailed in Section 4.2.
- `simulation/`: Hosts the core execution logic of the framework, including the discrete-time simulation engine (`engine.py`) and the `trip_manager.py` module responsible for operational scheduling and vessel assignment.
- `optimization/` **and** `prediction/`: Contain the algorithms used for energy management and predictive control. These modules implement the control strategies and predict generation mechanisms described in subsequent sections.
- `assets/`: Stores external static data required by the simulator, such as electricity tariff schedules and the vessel route files.

```
.
|-- assets/           # External data (tariffs, trip)
|-- config/           # Global settings and configuration
|-- database/         # SQL persistence layer managers
|-- prediction/       # Predictive models for load and PV
|-- models/           # Physical entity classes (Boat, PV, BESS)
|-- optimization/     # Energy management algorithms
|-- simulation/       # Core engine and event loop
|-- weather/          # OpenMeteo API integration
|-- main.py           # Simulation entry point
`-- streamlit_app.py  # Dashboard entry point
```

Listing 1: PyPort Sim project directory structure.

This modular organization directly supports the **Extensibility** and **Modularity** requirements by decoupling physical asset models, control algorithms, and execution logic into independent packages. As a result, new assets, forecasting approaches, or energy management strategies can be integrated through additional modules without requiring modifications to the simulation engine or existing components.

4.1.2 Database Structure

The data persistence layer of *PyPort Sim* is implemented using a **relational database**. While the system must handle time-indexed data efficiently, a relational database was chosen primarily for its transparency and ease of inspection during development and testing.

To accommodate the heterogeneous and evolving nature of the stored data, ranging from meteorological variables and electrical measurements to control set-points, the database adopts an Entity Attribute Value (EAV) data model [59]. In contrast to a classical relational schema, where each new asset or metric would require structural modifications and schema migrations, the EAV approach stores all time-varying data in a uniform, vertical format. This design choice allows the simulator to support an arbitrary number of devices and metrics without altering the underlying database structure.

The EAV model is particularly well suited to this application for three reasons. First, the set of simulated assets and metrics is not fixed and may evolve as new port configurations, devices, or control strategies are introduced. Second, the simulator prioritizes flexibility and extensibility over attaching strong semantic meaning to individual database columns. Finally, the performance overhead typically associated with EAV schemas is acceptable in this context, as the database is

used primarily for logging, post-simulation analysis, and visualization rather than high-frequency transactional workloads.

As illustrated in the Entity-Relationship (ER) diagram in Figure 7, the database architecture centers around two primary dimensional tables: `source` and `metric`. The `source` table defines the physical or virtual entities producing or associated with the data (e.g., specific vessels, chargers, PV systems, or weather stations), while the `metric` table catalogs the specific measurable quantities or statuses being recorded (e.g., state of charge, active power, temperature).

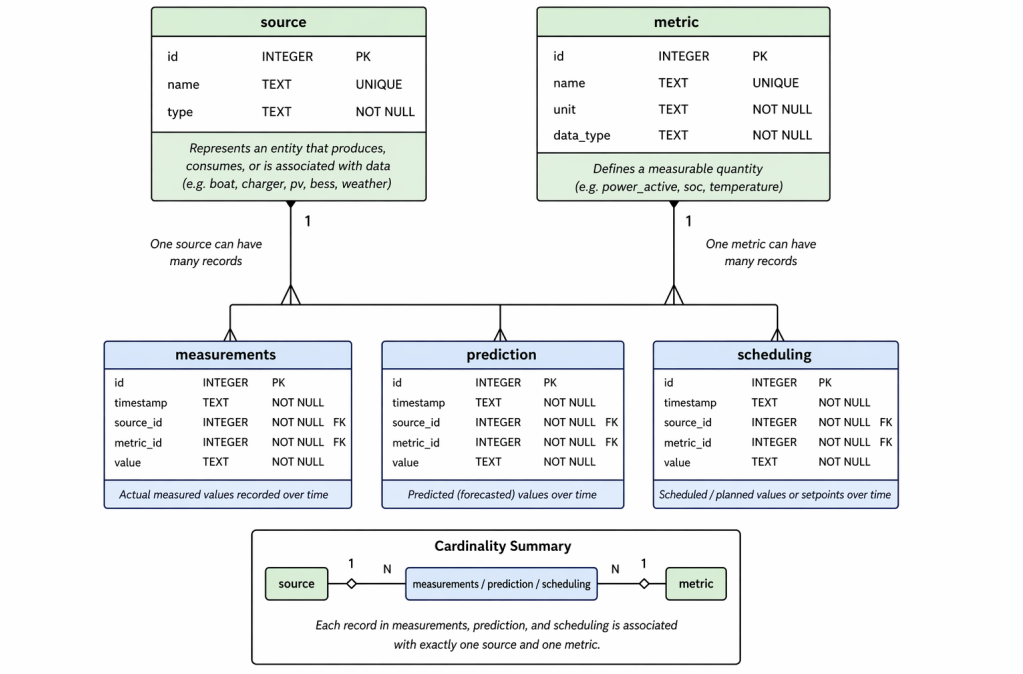

Figure. 7: Entity-Relationship (ER) diagram and cardinality.

These two parent tables establish a one-to-many relationship with three specialized temporal data tables. Through the use of foreign keys (`source_id` and `metric_id`), each time-series record is strictly associated with exactly one source and one metric.

- The `measurements` table stores the "ground-truth" values generated by the simulation engine at each timestep, representing the actual physical state of the system.

- The `prediction` table contains predictive data produced by the Prediction Module, such as weather variables retrieved from Open-Meteo or anticipated load profiles.

– The `scheduling` table records the control actions computed by the Optimization Module, corresponding to planned power set-points and operational decisions for controllable assets.

4.1.3 Visualization Interface

The simulation framework generates extensive, multi-dimensional time-series data stored across various tables. To simplify the analysis of this raw data, a lightweight visualization dashboard was developed. This interface allows users to inspect, validate, and export results directly, without needing to write custom SQL queries.

The development process began with a structural mock up aimed at organizing the user workflow into logical steps: database selection, data filtering, and visual rendering. As illustrated in Figure 8, the conceptual layout prioritizes a clean separation between global navigation on the left and the primary analytical workspace on the right.

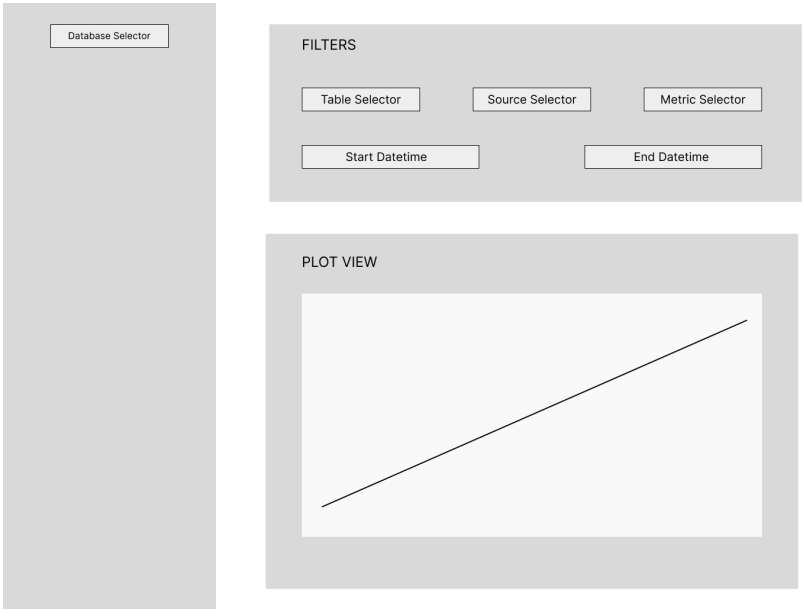

Figure. 8: Conceptual mock up of the visualization dashboard layout.

Following this design, the final application was implemented using `Streamlit` for the frontend architecture and `Plotly` for interactive data rendering (Figure 9). The interface operates in read-only mode, connecting directly to the output database layer to ensure data integrity during analysis.

To guide users through the data exploration process, the interface is systematically structured into three primary functional areas:

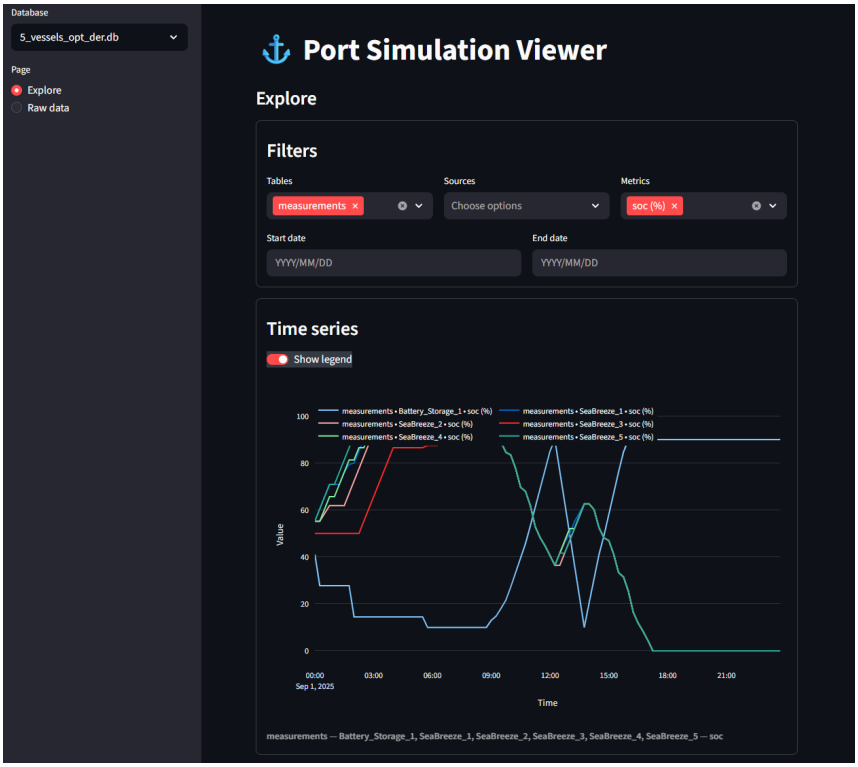

Figure. 9: Implemented Streamlit visualization dashboard.

– **Sidebar Navigation:** Located on the left, this panel acts as the entry point for analysis. Users first load a specific simulation database (e.g., `5_vessels_opt_der.db`). Below the database selector, users can toggle between the visual "Explore" mode and the tabular "Raw data" mode.

– **Filters Panel:** Situated at the top of the main workspace, this section enables granular data querying. Users can filter by the target table (`measurements`, `prediction`, or `scheduling`), specify one or multiple sources (e.g., individual vessels, battery storage systems), and select specific metrics to display (e.g., State of Charge, power exchange). Start and end date selectors further narrow the temporal scope of the analysis.

– **Data View:** The bottom section dynamically responds to the applied filters. In the "Explore" page, time-series visualizations are generated, plotting one distinct trace per combination of table, source, and metric. The interactive nature of the plot allows users to hover for exact values, zoom into specific time frames, and toggle the legend. Alternatively, when navigating to the "Raw data" page, this space displays a comprehensive data table, enabling direct tabular inspection and CSV export of the selected records for external post-processing.

4.2 Models of Port Assets

This section describes the modeling approach for the core entities: electric vessels, charging infrastructure, renewable generation, and storage.

4.2.1 Recreational Vessel

As established in Section 2.3.1, the energy consumption of recreational vessels is strongly non-linear and dominated by hydrodynamic resistance. In displacement and semi-planing regimes, the dominant resistive forces scale approximately with the square of the vessel speed, resulting in a propulsion power demand that grows cubically with speed. This relationship is commonly referred to as the *Propeller Law* or *Cube Law*, which states that the required propulsion power is proportional to the cube of the vessel velocity [60].

Listing 2 illustrates the instantiation of a recreational vessel within the simulation topology. The `Boat` class encapsulates the minimum set of physical and energetic parameters required to evaluate propulsion power demand, battery depletion, and charging behavior. These parameters are directly used in the mathematical model or required to enforce physical feasibility and operational constraints.

```
boat1 = Boat(
    name="SeaBreeze",
    motor_power=120,        # Rated motor power (kW)
    weight=2500,            # Displacement (kg)
    length=8.5,             # Hull length (m)
    battery_capacity=150,   # Total energy capacity (kWh)
    range_speed=15.0,       # Range speed (knots)
    soc=0.30,               # Initial State of Charge (30%)
)
```

Listing 2: Instantiation of a recreational vessel model.

The `motor_power` and `range_speed` parameters define a characteristic operating point of the vessel and are used to calibrate its propulsion model. The `battery_capacity` directly determines the vessel's usable energy storage and governs the evolution of the state of charge. The `soc` variable represents the vessel's initial energetic state. The remaining geometric parameters, `weight` and `length`, are validated to ensure physical consistency and are retained to enable future model refinements, such as resistance-based scaling or hull-dependent corrections.

The core of the propulsion model is the derivation of a vessel-specific proportionality coefficient, denoted as k, which characterizes the relationship between speed and propulsion power demand. Adapted from the cubic relationship established by [29], this coefficient is computed during object initialization using the vessel's rated motor power P_{rated} and its nominal range speed v_{range}:

$$k = \frac{P_{\text{rated}}}{v_{\text{range}}^3} \tag{2}$$

During simulation, the instantaneous propulsion power demand $P_{\text{dem}}(t)$ is evaluated dynamically as a function of the vessel speed $v(t)$, which is obtained from the trip telemetry data, following the established Cube Law for vessel propulsion [29]:

$$P_{\text{dem}}(t) = k \cdot v(t)^3 \tag{3}$$

The evolution of the battery state of charge (SOC) is modeled through a discrete-time energy balance using the standard Coulomb counting method [61]. At each simulation timestep Δt, expressed in seconds, the energy consumed by propulsion is computed and normalized by the total battery capacity C_{batt}, expressed in kilowatt-hours. The conversion factor of 3600 accounts for the unit transformation between seconds and hours. During a discharging phase, the SOC update is given by:

$$SOC(t+1) = SOC(t) - \frac{P_{\text{dem}}(t) \cdot \Delta t}{3600 \cdot C_{\text{batt}}} \tag{4}$$

Conversely, when the vessel is connected to a charger at the port, the SOC increases according to the charging power $P_{\text{charger}}(t)$ and the charging efficiency η:

$$SOC(t+1) = SOC(t) + \frac{P_{\text{charger}}(t) \cdot \eta \cdot \Delta t}{3600 \cdot C_{\text{batt}}} \tag{5}$$

4.2.2 Recreational Trips

To ensure the simulation reflects realistic operational scenarios, the trips in *PyPort Sim* are grounded in empirical data rather than random coordinates. They were derived from real-world

data collected from the Marina of Funchal. The dataset was obtained from MarineTraffic[3], focusing on a representative recreational vessel that frequently operates in the area.

1. Data Acquisition and Cleaning: The raw dataset initially covered a broad temporal range, however, a significant portion of the days contained no movement data. After filtering for days with valid activity, 8 distinct route profiles were identified. As illustrated in Figure 10, the raw telemetry data presented several inconsistencies not suitable for direct simulation usage:

- **Discontinuities:** Large time gaps between GPS points resulted in "teleportation" like behavior.
- **Incomplete Trajectories:** Several routes did not originate or terminate at the designated berth coordinates.
- **Physical Violations:** Simple linear interpolation between points occasionally resulted in paths crossing physical port infrastructure, specifically, the breakwaters.

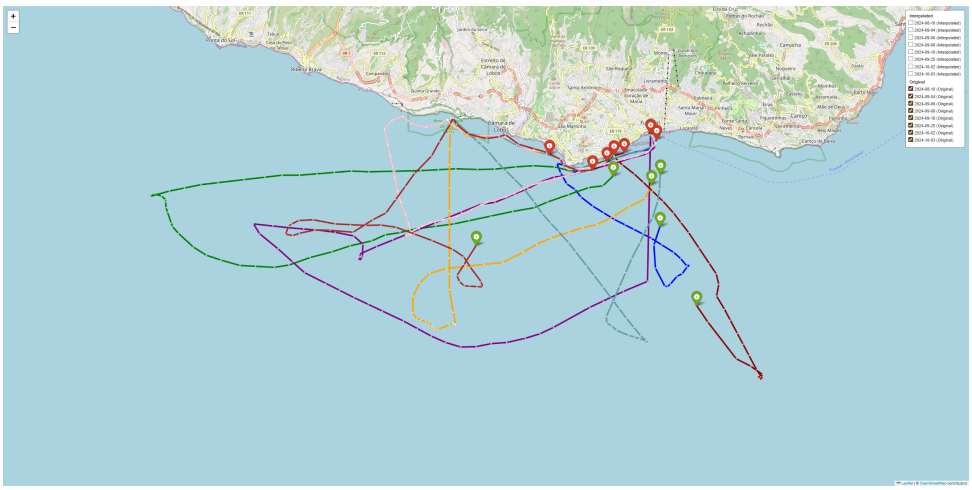

Figure. 10: Original raw GPS traces showing gaps and inconsistent start/end points.

2. Route Processing Pipeline: To resolve these issues, a custom processing pipeline was implemented to normalize and repair the trajectories. The algorithm performs two key operations:

- **Interpolation:** To address data discontinuities, the system fills gaps between consecutive points using distance calculations. If the distance between two telemetry points exceeds a defined threshold, 200 meters, the algorithm generates intermediate coordinates, effectively smoothing the path and preventing sudden jumps in vessel speed or location.

[3] `https://www.marinetraffic.com`

– **Topology Constraints:** To prevent vessels from "clipping" through port breakwaters, a fixed-path mechanism was implemented. The system enforces a mandatory, collision-free sequence of way-points for all departures and arrivals. The algorithm identifies the start and end points of a trip and automatically appends this static path.

3. Processed Results: The result of this pipeline is a set of continuous, physically valid trajectories. As shown in Figure 11, the vessels now correctly navigate the port channel before merging into their historical routes.

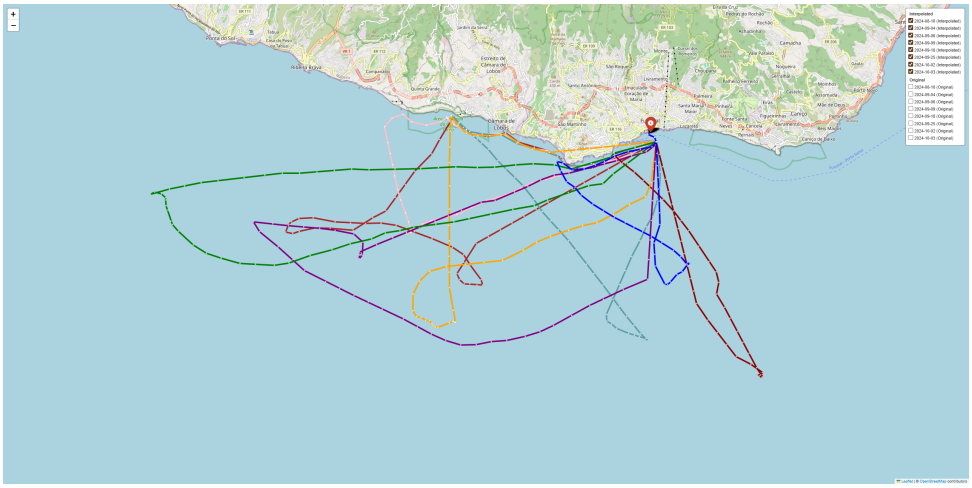

Figure. 11: Interpolated routes with fixed port entry/exit sequences.

The final processed routes are serialized into CSV format for consumption by the *Trip Manager*. Each entry includes the timestamp, speed, heading, and coordinates.

4.2.3 EVSE

The Electric Vehicle Supply Equipment (EVSE), or charger, is modeled as a unidirectional, state-aware actuator responsible for regulating the power transfer between the port microgrid and a connected vessel. Each charger is characterized by a rated maximum output power $P_{\max}^{EVSE}$ and a conversion efficiency factor $\eta_{evse} \in [0, 1]$, representing AC/DC conversion losses. The charger operates strictly in charging mode and does not support bidirectional power flow, in other words, negative power values are not allowed by the model.

Listing 3 illustrates the instantiation of a standard charging station within the simulation framework.

```
charger1 = Charger(
    name="Charger_01",
    max_power=22,          # Maximum output power (kW)
    efficiency=0.95        # AC/DC conversion efficiency (95%)
)
```

Listing 3: Instantiation of a Charger model.

At each simulation timestep t, the charger exposes a power set-point $P_{out}(t)$ determined by the energy management system. This set-point represents the electrical power drawn from the grid or local microgrid at the charger terminals. The model enforces strict hardware constraints to ensure physical feasibility, a standard formulation in microgrid energy management [62]:

$$0 \leq P_{out}(t) \leq P_{\max}^{EVSE} \tag{6}$$

The charger implementation assumes that upstream control logic, either the rule-based controller or the optimization, respects this bound before assigning the set-point. The effective power delivered to the vessel battery accounts for conversion losses and is computed internally as:

$$P_{eff}(t) = P_{out}(t) \cdot \eta_{evse} \tag{7}$$

Thus, $P_{out}(t)$ corresponds to grid-side power, while $P_{eff}(t)$ represents the battery-side charging power. Over a discrete timestep Δt, the energy transferred to the vessel battery is given by:

$$E_{delivered}(t) = \frac{P_{out}(t) \cdot \eta_{evse} \cdot \Delta t}{3600} \quad [\text{kWh}] \tag{8}$$

Functionally, the `Charger` class operates as a finite state machine with two primary states: `IDLE` and `CHARGING`. In the `CHARGING` state, a vessel is connected and a strictly non-negative power set-point is applied. When the state transitions to `IDLE`, either because the charging session is complete or because the vessel has physically departed the berth, the implementation automatically resets the power output to zero and clears the reference to the connected vessel.

Within the overall port topology, multiple chargers are aggregated inside the `Port` container. Either the rule-based engine or, when enabled, the Optimization Module computes the power schedule $P_{out,i}(t)$ for each charger i, ensuring compliance with the rated limit $P_{\max}^{EVSE}$. The Simu-

lation Engine then applies these set-points at each timestep to update vessel battery states using the effective charging power $P_{eff}(t)$.

4.2.4 PV System

The PV model represents the primary renewable generation source within the port microgrid. The implementation relies on the `pvlib` Python library to compute solar position, plane-of-array irradiance, cell temperature, and DC power output using physically validated models.

Listing 4 shows the instantiation of a PV array.

```
pv_system = PV(
    name="solar_1",
    capacity=50.0,        # Rated DC capacity (kW at STC)
    tilt=30.0,            # Panel tilt angle (degrees)
    azimuth=180.0,        # South-facing orientation (degrees)
    latitude=32.64,       # Location: Funchal
    longitude=-16.90
)
```

Listing 4: Instantiation of the PV generation model.

The parameter `capacity` represents the DC nameplate power at Standard Test Conditions (STC), defined at an irradiance of 1000 W/m^2 and a cell temperature of 25°C. The orientation of the array is defined by the tilt angle β and the azimuth angle, following the `pvlib` convention (180° corresponds to south-facing in the northern hemisphere).

For each simulation timestep, the method `calculate_production(...)` is called using the timestamp and meteorological inputs, such as GHI, DNI, DHI. The production calculation follows a sequential physical modeling chain:

First, the solar position is computed using `get_solarposition`, which determines the apparent elevation and azimuth angles of the sun based on the geographic coordinates and timestamp. If the apparent solar elevation is less than or equal to zero, sun below horizon, the instantaneous production is set to zero.

Second, the Plane-of-Array (POA) irradiance is calculated using `get_total_irradiance`. This function transposes the horizontal irradiance components (GHI, DNI, DHI) to the tilted module surface using, resulting in the total incident irradiance G_{POA}.

Third, the photovoltaic cell temperature is estimated using the temperature model `sapm_cell`, which accounts for POA irradiance, ambient temperature, and wind speed. This step captures thermal efficiency losses due to increased cell temperature.

Finally, the DC power output is computed using the PVWatts model via `pvwatts_dc`[4]. The model evaluates:

$$P_{DC}(t) = P_{dc0} \cdot \frac{G_{POA}(t)}{1000} \left[1 + \gamma \left(T_{cell}(t) - 25°C\right)\right] \tag{9}$$

where P_{dc0} corresponds to the rated DC capacity at STC, γ is the temperature coefficient of power, and T_{cell} is the estimated cell temperature. The resulting power is converted to kilowatts and clipped to ensure non-negative output.

The instantaneous generation is stored in the attribute `power_production` and returned to the simulation engine. At the system level, the total renewable generation is obtained by summing the production of all PV instances within the `Port` container at each timestep.

4.2.5 BESS

The BESS acts as the primary flexibility buffer within the port microgrid. It is modeled as a controllable bidirectional active power device capable of both consuming and supplying energy. Listing 5 presents the instantiation of the storage unit, defining its energy capacity, power ratings, efficiency, and operational limits.

```
bess = BESS(
    name="bess_1",
    capacity=200.0,           # Total energy capacity (kWh)
    max_charge_power=50.0,    # Max charging rate (kW)
    max_discharge_power=50.0, # Max discharging rate (kW)
    efficiency=0.90,          # Efficiency factor
    soc_min=0.10,             # Minimum State of Charge (10%)
    soc_max=0.90,             # Maximum State of Charge (90%)
    initial_soc=0.50          # Start simulation at 50%
)
```

Listing 5: Instantiation of the Battery Energy Storage System model.

[4] https://pvlib-python.readthedocs.io/en/latest/reference/generated/pvlib.pvsystem.pvwatts_dc.html

The parameter `capacity` represents the total usable energy in kWh. The state of charge $SOC(t) \in [SOC_{\min}, SOC_{\max}]$ is expressed in per-unit form and initialized at `initial_soc`. The efficiency parameter η is applied symmetrically during charging and discharging. Consequently, charging multiplies stored energy by η, while discharging divides delivered energy by η.

During a charging event with requested power $P_{charge}(t)$, the model first limits the set-point to the hardware constraint:

$$P_{charge}(t) \leq P_{\max}^{charge} \tag{10}$$

The energy stored in the battery over a timestep Δt is:

$$E_{added} = P_{charge}(t) \cdot \frac{\Delta t}{3600} \cdot \eta \tag{11}$$

and the state of charge is updated following the Coulomb counting method [61] as:

$$SOC(t+1) = SOC(t) + \frac{E_{added}}{C_{cap}} \tag{12}$$

If this update would exceed $SOC_{\max}$, the charging power is automatically reduced so that $SOC(t+1) = SOC_{\max}$ exactly.

Similarly, during discharging with requested power $P_{dis}(t)$, the power is limited to:

$$P_{dis}(t) \leq P_{\max}^{dis} \tag{13}$$

The energy delivered to the grid or loads is:

$$E_{delivered} = P_{dis}(t) \cdot \frac{\Delta t}{3600} \tag{14}$$

Due to conversion losses, the energy removed from the battery is:

$$E_{removed} = \frac{E_{delivered}}{\eta} \tag{15}$$

and the state update becomes [61]:

$$SOC(t+1) = SOC(t) - \frac{E_{removed}}{C_{cap}} \tag{16}$$

If this update would violate $SOC_{\min}$, the discharging power is reduced such that the battery reaches exactly $SOC_{\min}$.

To support higher-level control decisions, the model exposes helper methods that compute the available discharge energy and available charging capacity, as well as the maximum feasible power for the current timestep.

By default, the BESS operates under a conservative rule-based control strategy. When integrated with photovoltaic generation, the battery prioritizes absorbing surplus PV production and discharges only when the net demand exceeds the contracted grid limit. In grid-only scenarios, charging is performed during low-demand periods and discharging is triggered solely to prevent grid constraint violations.

4.3 Simulation Logic and Algorithms

This section delineates the computational workflow that drives the simulation. While the mathematical models defined previously describe the physical behavior of individual assets, the simulation logic orchestrates their interaction over time.

4.3.1 Configuration

The configuration architecture of *PyPort Sim* is structured into three layers that separate global parameters, system topology, and external data sources.

1. Global Simulation Context: Global runtime parameters are encapsulated in a dedicated `Settings` dataclass located in `settings.py`, as shown in Listing 6. This object defines the simulation timestep Δt (in seconds), execution mode, database path, and behavioral flags controlling optimization and power-limiting logic. It also specifies the daily trip departure schedule as ordered pairs.

```
class SimulationMode(Enum):
    REAL_TIME = "real_time"
    BATCH = "batch"
```

```
4
5  @dataclass
6  class Settings:
7      timestep: int = 900                  # Simulation step (seconds)
8      mode: SimulationMode = SimulationMode.BATCH
9      db_path: str = "port_simulation.db"
10     use_optimizer: bool = False
11     power_limit_mode: bool = False
12     trip_schedule: tuple = ((9, 0), (14, 1))
```

Listing 6: Global simulation settings dataclass.

The parameter `use_optimizer` determines whether `Charger` and `BESS` schedules are computed via the optimization module or via rule-based control. The `power_limit_mode` flag enables enforcement of contracted grid limits without invoking the optimizer, providing a baseline operational scenario for comparison.

2. Topology Definition: The physical configuration of the port is defined manually in `main.py`. System components (`Boat`, `Charger`, `PV`, `BESS`) are instantiated as native Python objects and aggregated into a `Port` container.

3. External Assets: Operational data such as recreational routes and tariff definitions are stored externally in the `assets/` directory (CSV and JSON formats). These files are loaded dynamically at runtime.

4.3.2 Trip Manager

The *Trip Manager* is responsible for loading recreational route definitions and assigning daily trips to vessels. It provides an abstraction layer between static CSV route files and the dynamic execution of trips within the simulation engine.

Route definitions are stored as CSV files in the `assets/trips` directory using the naming convention `route_*.csv`. Each file contains a time-ordered sequence of waypoints with the structure shown in Listing 7.

```
1  timestamp,type,speed,heading,latitude,longitude
2  2024-10-03 09:03:21.560000,Static,0.0,0.0,32.64542,-16.90841
3  ...
```

Listing 7: Structure of a trip route CSV file.

Each row represents a vessel state at a given timestamp, where `speed` is expressed in knots and geographic coordinates are provided in decimal degrees.

Upon loading, each CSV file is wrapped into a `Trip` object (Listing 9), which internally stores an ordered list of `TripPoint` instances (Listing 8). A `TripPoint` represents a single sampled waypoint along the route.

```
@dataclass
class TripPoint:
    timestamp: datetime
    point_type: str
    speed: float         # knots
    heading: float       # degrees
    latitude: float
    longitude: float
```

Listing 8: TripPoint dataclass.

```
class Trip:
    def __init__(self, csv_path: str):
        self.route_name = Path(csv_path).stem
        self.points: List[TripPoint] = []
        self._load_from_csv(csv_path)

        if self.points:
            first_time = self.points[0].timestamp
            last_time = self.points[-1].timestamp
            self.duration = (last_time - first_time).total_seconds()
        else:
            self.duration = 0
```

Listing 9: Trip class initialization and structure.

The `Trip` object parses the CSV file, constructs a sequence of `TripPoint` elements, and computes the total trip duration as the time difference between the first and last waypoint.

Energy consumption along the route is derived using the same cubic propulsion model introduced in Section 4.2.1. For each segment between consecutive waypoints, the instantaneous propulsion power is evaluated as $P = k \cdot v^3$, and energy is obtained by integrating over the segment duration.

Daily trip assignment follows a semi-deterministic policy. For each boat and simulation date, the number of trips is determined based on the weekday:

– Monday–Friday: two trips,

– Saturday: one trip,

– Sunday: no trips.

For each day, the required number of trips is selected randomly from the set of available routes. When enough distinct routes exist, the selection is made without repetition; otherwise, routes may be reused to satisfy the required number of trips. At the start of each simulation day, the engine requests the daily assignments from the Trip Manager. Later, at each scheduled departure time defined in the global settings, the engine retrieves the corresponding route for that time slot. During navigation, the engine queries the `Trip` object to compute the energy consumed over the current timestep, ensuring that the vessel's battery discharge accurately reflects the propulsion demand of the selected route.

4.3.3 Prediction

The *Prediction Module* generates a 24-hour prediction of renewable production and vessel charging requirements. For a given prediction date, it produces a sequence of time-indexed `EnergyPrediction` objects, each representing the expected system state at a discrete timestep Δt.

The core data structure is shown in Listing 10.

```
@dataclass
class EnergyPrediction:
    timestamp: datetime
    power_active_production_kw_by_source: Dict[str, float]
    power_active_production_kw: float
    boat_required_energy_kwh: Dict[str, float]
    boat_available: Dict[str, int]
```

Listing 10: EnergyPrediction data structure.

Each prediction entry contains PV active power production per source and aggregated at port level (kW), required energy per boat until its next scheduled departure (kWh), and a binary availability indicator (1 = available to charge, 0 = not available).

Weather Data Service:

Meteorological data are retrieved via a dedicated Open-Meteo client, which automatically selects between the forecast API and the historical archive API depending on the requested date. If the forecast start date precedes the current day, the archive endpoint is used; otherwise, the standard forecast endpoint is queried.

Hourly weather variables such as Global Horizontal Irradiance (GHI), Direct Normal Irradiance (DNI), Diffuse Horizontal Irradiance (DHI), and ambient temperature are parsed and stored in the database under the `prediction` table. The `PortPredictor` subsequently retrieves these records for the requested date and uses them as inputs to the PV production model.

PV Production Prediction:

For each timestep, the predictor evaluates the expected PV generation by calling the method `calculate_production(...)` of every `PV` instance in the port. The prediction uses the hourly weather data retrieved from the database and computes instantaneous active power (kW) per PV unit, as well as the aggregated port-level production. If no PV systems are defined, the predicted production defaults to zero.

Boat Energy Requirement Prediction:

For each vessel, the module determines the next scheduled departure using the configured daily departure times and the trip assignments provided by the Trip Manager. If a future departure exists, the required propulsion energy is estimated using:

$$E_{\text{required}} = \texttt{Trip.estimate\_energy\_required}(k)$$

where k is the vessel-specific propulsion coefficient. If no further departures are scheduled for that day, the required energy is set to zero.

Boat Availability Prediction:

Boat availability is computed as a binary state derived from two conditions: the vessel must not be currently sailing, and the current timestamp must lie within a valid charging window, this is before the first trip, between trips, or after the last arrival. The resulting indicator is used by the optimization module to constrain charging decisions.

The complete 24-hour sequence of `EnergyPrediction` objects is returned to the simulation engine and persisted in the database. These time-series values constitute the inputs of the optimization problem, namely predicted renewable generation $P_{pv}^{est}(t)$, vessel energy requirements, and vessel charging availability constraints.

4.4 Optimization Module

The *Optimization Module* generates a day-ahead charging schedule that minimizes operational costs while ensuring technical feasibility with respect to grid limits, vessel energy requirements, and BESS constraints. The scheduling problem is formulated as a MILP and solved using the Solving Constraint Integer Programs (SCIP) solver through the `PySCIPOpt` interface. The optimization horizon is discretized into T equally spaced timesteps, each of duration $\Delta t = 900$ seconds (15 minutes). To ensure numerical stability and computational efficiency, the solver was configured with a relative gap tolerance of 1% and a strict time limit of 120 seconds.

4.4.1 Sets and Parameters

We define the set of timesteps $\mathcal{T} = \{0, \ldots, T-1\}$, the set of vessels $\mathcal{V}$, the set of chargers $\mathcal{C}$, and the set of BESS units $\mathcal{S}$. For each vessel $v \in \mathcal{V}$, a set of requested trips $\mathcal{K}_v$ is derived from the availability prediction. Each trip $k \in \mathcal{K}_v$ is characterized by a departure deadline t_d, a required energy amount E_{req} that must be available at departure, and a trip duration D.

To provide operational flexibility and avoid unnecessary trip cancellations, the model allows delayed departures. For each trip k, a set of feasible departure delay options is defined as $\Omega_{v,k} = \{0, \ldots, S_{max}\}$, where $s = 0$ corresponds to an on-time departure and larger values of s represent increasing delay. In this implementation, the maximum delay S_{max} was set to 8 timesteps (equivalent to 2 hours). This bounds passenger inconvenience while offering sufficient flexibility to the solver to shift loads away from power peaks.

4.4.2 Decision Variables

The model uses continuous variables to represent power flows and energy states, and binary variables to model discrete trip scheduling decisions. A detailed overview of all decision variables is provided in Table 1.

Variable	Description
$P_{grid}(t)$	Grid import power at time t [kW]
$P_{ch,c}(t)$	Power set-point for charger $c \in \mathcal{C}$ [kW]
$P_{b,ch}(t)$	Charge power for BESS $b \in \mathcal{S}$ [kW]
$P_{b,dis}(t)$	Discharge power for BESS $b \in \mathcal{S}$ [kW]
$E_b(t)$	Energy stored in BESS b [kWh]
$E_v(t)$	Energy stored in vessel v battery [kWh]
$P_{export}(t)$	Slack variable for excess production (curtailment/export) [kW]
Binary Variables	
$\delta_{v,k,s}$	Equals 1 if vessel v departs for trip k with delay s
$\gamma_{v,k}$	Equals 1 if trip k is executed (not missed)

Table 1: Decision Variables

4.4.3 Objective Function

The objective function J aims to minimize total operational cost while maintaining a high level of service quality. Rather than evaluating isolated goals, it consists of four unified components that balance economic efficiency, service performance, and battery health:

$$\min J = C_{energy} - R_{service} + \Phi_{miss} + \Phi_{bess} \tag{17}$$

The first term, **Energy Cost (C_{energy})**, represents the total cost of importing electricity from the grid. Because the imported power $P_{grid}(t)$ is expressed in kW, the time-varying tariff $\pi(t)$ in €/kWh, and Δt in seconds, a conversion factor of 3600 is introduced to align the time units to hours:

$$C_{energy} = \sum_{t \in \mathcal{T}} P_{grid}(t) \cdot \pi(t) \cdot \frac{\Delta t}{3600} \tag{18}$$

The second term, **Service Reward ($R_{service}$)**, grants a reward for every successfully executed trip. To encourage punctual departures, the reward decreases exponentially with delay s:

$$R_{service} = \sum_{v \in \mathcal{V}} \sum_{k \in \mathcal{K}_v} \sum_{s \in \Omega_{v,k}} (\alpha \cdot \beta^s) \cdot \delta_{v,k,s} \tag{19}$$

Here, α denotes the base reward for an on-time trip, set to 1000.0 to establish a high baseline value for trip execution. The parameter $\beta \in (0, 1)$ is a decay factor, set to 0.5. This steep penalization

reduces the reward by half for each subsequent 15-minute delay slot, strongly driving the solver to prioritize punctuality.

The third term, **Missed Trip Penalty (Φ_{miss})**, imposes a large penalty if a trip is not executed, acting as a soft constraint to discourage cancellations. The penalty M_{trip} was set to 2000, double the base reward α. This guarantees that the solver will always prefer scheduling a trip, even at maximum delay, over canceling it outright.

$$\Phi_{miss} = \sum_{v \in \mathcal{V}} \sum_{k \in \mathcal{K}_v} M_{trip} \cdot (1 - \gamma_{v,k}) \tag{20}$$

The final term, **BESS Degradation Penalty (Φ_{bess})**, limits excessive depletion of the storage units by the end of the optimization horizon. It penalizes scenarios where the final State of Charge (SOC) at $t = T$ falls below its initial value at $t = 0$, multiplied by a tuning weight W_{bess} (set to 0.5):

$$\Phi_{bess} = W_{bess} \cdot \sum_{b \in \mathcal{S}} \max\left(0, E_b(0) - E_b(T)\right) \tag{21}$$

The choice of $W_{bess} = 0.5$ applies a gentle penalty relative to the grid cost, allowing the BESS to be utilized for peak shaving during the day while encouraging the system to replenish its reserves using excess renewable generation before the horizon ends.

4.4.4 Constraints

1. Grid and Power Balance: The grid import is limited by the contracted power capacity P_{cont}. System-wide power balance is enforced through a strict equality constraint at every timestep. The slack variable $P_{export}(t)$ absorbs excess generation (e.g., PV surplus), which allows the use of an equality instead of an inequality. This typically improves the tightness of the Linear Programming (LP) relaxation and enhances solver performance:

$$P_{grid}(t) + P_{PV}(t) + \sum_{b \in \mathcal{S}} P_{b,dis}(t) = \sum_{c \in \mathcal{C}} P_{ch,c}(t) + \sum_{b \in \mathcal{S}} P_{b,ch}(t) + P_{export}(t) \tag{22}$$

2. Trip Scheduling and Logic: For each trip, at most one departure time (including delays) can be selected. The binary variable $\gamma_{v,k}$ links the departure decision to the execution status of

the trip:

$$\sum_{s \in \Omega_{v,k}} \delta_{v,k,s} = \gamma_{v,k} \leq 1 \tag{23}$$

3. Vessel Availability (At-Sea Logic): A vessel cannot charge while it is at sea. An auxiliary state variable $A_v(t)$ indicates whether vessel v is away at time t. This state is derived from the selected departure decisions and trip durations. Charging power is therefore restricted to periods when the vessel is docked:

$$P_{ch,c}(t) \leq P_c^{max} \cdot (1 - A_v(t)) \tag{24}$$

4. Vessel SOC and Tight Big-M: To guarantee operational feasibility, the vessel's SOC at the actual departure time ($t_d + s$) must be at least equal to the required trip energy E_{req}. This condition is enforced using a Big-M formulation. To ensure numerical stability and improve branch-and-bound performance, the Big-M parameter M is tightly defined as the exact required energy for the specific trip ($M = E_{req}$), rather than an arbitrarily large number or the full battery capacity:

$$E_v(t_d + s) \geq E_{req} - M \cdot (1 - \delta_{v,k,s}) \tag{25}$$

5. BESS Dynamics: The energy evolution of each storage unit follows standard inventory dynamics. Charging and discharging efficiencies (η) are explicitly considered. As with the cost function, Δt is converted to align the power variables [kW] with the energy capacity units [kWh]:

$$E_b(t) = E_b(t-1) + \left(P_{b,ch}(t) \cdot \eta - \frac{P_{b,dis}(t)}{\eta} \right) \frac{\Delta t}{3600} \tag{26}$$

This constraint ensures physically consistent SOC evolution across the planning horizon, accounting for conversion losses during both charging and discharging phases.

4.5 Simulation Engine

The `SimulationEngine`, acts as the central orchestration layer of *PyPort Sim*. While previous sections detailed individual asset models, prediction, and optimization logic, the engine is responsible for coordinating their interaction within a unified discrete-time framework.

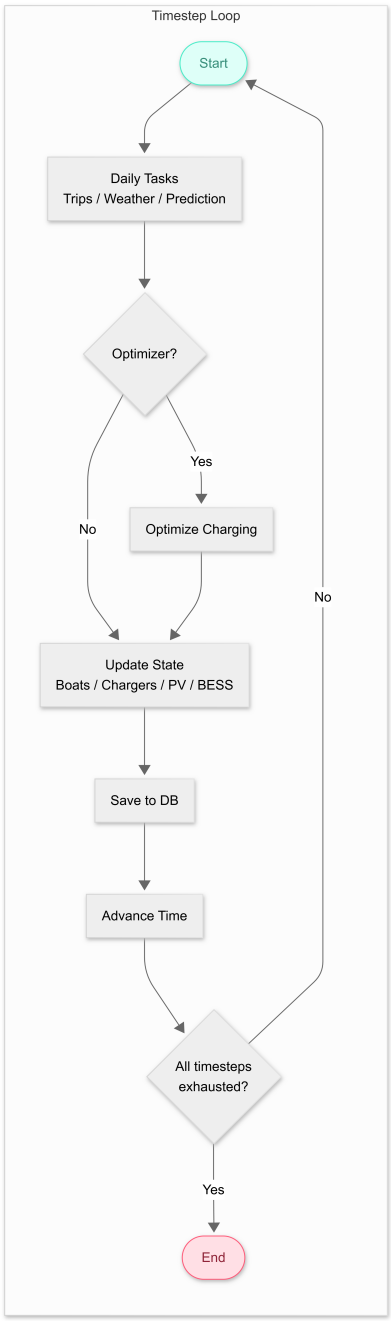

Figure. 12: High-level execution flow of the Simulation Engine.

As illustrated in Figure 12, the simulation clock advances in fixed increments of Δt until the predefined horizon is reached.

At each timestep, the engine executes a strictly ordered sequence to preserve physical causality:

1. **Daily tasks (midnight trigger):** weather forecast refresh, trip assignment via the `TripManager`, and generation of the 24-hour port energy prediction. If enabled, the optimization module is executed at this stage and the resulting schedules are stored in the database.
2. **Trip handling:** vessels transition between `IDLE`, `CHARGING`, and `SAILING` states. Propulsion energy is deducted using the cubic power model, and delayed departures are managed according to SOC feasibility.
3. **Renewable update:** PV production is computed from current meteorological conditions.
4. **Charging control:** boats are assigned to chargers according to either optimized schedules or rule-based strategies.
5. **BESS update:** storage units follow either scheduled set-points or default PV-coupled control logic.
6. **State persistence:** all power flows and asset states are written to the database.

The sequential structure ensures that physical states are updated, and that energy balances remain consistent at every timestep.

5 Evaluation Methodology

This chapter outlines the methodology used to validate the *PyPort Sim* environment. The methodology is divided into two phases: a bottom-up verification of individual software components and a comprehensive system-level assessment through defined case studies.

5.1 Unit Testing

To ensure the reliability and correctness of the simulation engine, a structured verification strategy was adopted based on the V-model framework. As illustrated in Figure 13, this approach emphasizes that verification and validation (V&V) are not isolated activities performed at the end of development, but continuous processes that accompany each stage of the system life-cycle.

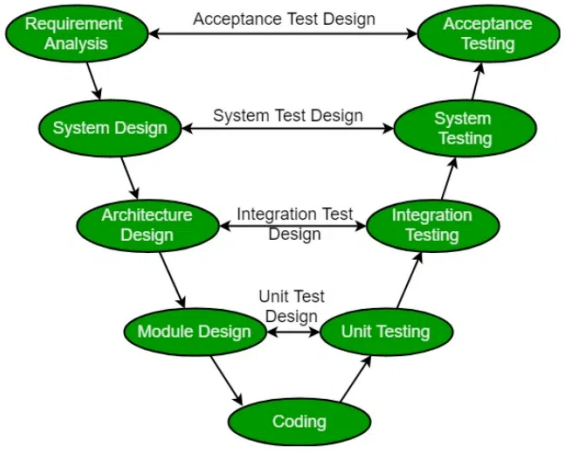

Figure. 13: V-model approach to system verification and validation.

Within the V-model structure, the left branch represents the progressive refinement of system requirements into detailed design specifications and implementable components, while the right branch mirrors this decomposition through corresponding verification and validation activities [63]. Unit testing, integration testing, and system validation are therefore directly linked to earlier specification stages.

In the context of *PyPort Sim*, the first verification layer focuses on the atomic correctness of the individual physical models described in Chapter 4, namely the Vessel, Charger, PV, and BESS

components. Each model is evaluated independently under controlled operating conditions to verify compliance with its expected behaviors.

5.1.1 Vessel Model Verification

The verification of the `Boat` class focuses on validating the correct implementation of the propeller law coefficient and the enforcement of physical constraints.

- **Objective:** Verify the correct computation of the hydrodynamic coefficient k and the enforcement of constructor validation rules.
- **Test Case 1 – Propeller Law Coefficient:** A vessel is initialized with predefined parameters ($P_{motor} = 500$ kW and $v_{range} = 10$ knots). The coefficient is computed internally as:

$$k = \frac{P_{motor}}{v_{range}^3}$$

  The analytical reference value ($k = 0.5$) is used to validate numerical correctness. The cubic scaling relation $P = kv^3$ is also evaluated externally for multiple speed values to confirm consistency.
- **Test Case 2 – Physical Boundary Conditions:** The model is instantiated with non-physical inputs, for example, non-positive motor power, invalid battery capacity, or $SOC \notin [0, 1]$. The expected behavior is that the class raises appropriate exceptions.
- **Test Case 3 – State Management:** The state setter is tested to ensure that only valid enumerated states (*IDLE*, *CHARGING*, *SAILING*) are accepted.

5.1.2 Charger Model Verification

The verification of the `Charger` class focuses on validating power constraints, efficiency handling, and operational state transitions.

- **Objective:** Verify that the charger enforces its rated power limits, correctly applies efficiency losses, and maintains consistent operational states.
- **Test Case 1 – Power Constraints:** The charger is initialized with a maximum power rating (P_{max}). The constructor is tested to ensure that invalid configurations raise exceptions. During

operation, requested power values exceeding P_{max} are externally clamped, and the assigned power is verified to remain within allowable limits.

– **Test Case 2 – Efficiency Handling:** The effective charging power delivered to the battery is evaluated using:

$$P_{\text{effective}} = P \cdot \eta_{evse}$$

The returned value is compared against reference calculations for different power levels to confirm correct loss modeling.

– **Test Case 3 – State Transitions:** The state setter is tested to ensure that only valid enumerated states (*IDLE*, *CHARGING*) are accepted. Additionally, transitions to the *IDLE* state are verified to automatically reset the output power and disconnect any associated vessel.

5.1.3 PV Model Verification

The verification of the `PV` class focuses on validating solar geometry calculations, irradiance-to-power conversion, and operational boundary conditions.

– **Objective:** Verify correct solar elevation computation, zero production during night hours, realistic diurnal production behavior, and enforcement of rated capacity limits.

– **Test Case 1 – Night Condition:** For timestamps where the apparent solar elevation satisfies $\alpha \leq 0$, the model is expected to return zero power output. Multiple night-time hours are evaluated to confirm consistent behavior.

– **Test Case 2 – Diurnal Production Profile:** A clear-sky day is simulated using representative irradiance inputs. The resulting production profile is evaluated to confirm a bell-shaped curve during daylight hours, with peak generation occurring near solar noon.

– **Test Case 3 – Capacity Constraint:** The instantaneous production is verified to never exceed the rated DC capacity of the system.

5.1.4 BESS Model Verification

The verification of the `BESS` class focuses on validating charging and discharging dynamics, efficiency modeling, power limits, and SOC boundary enforcement.

– **Objective:** Verify correct energy balance during charging and discharging, enforcement of maximum power limits, and compliance with SOC constraints.

– **Test Case 1 – Charging Dynamics:** The battery is initialized at a defined SOC and subjected to a charging command at rated power for a known timestep. The stored energy is evaluated using:

$$E_{\text{stored}} = P_{\text{charge}} \cdot \eta \cdot \Delta t$$

The resulting SOC variation is compared against the analytical expectation.

– **Test Case 2 – Discharging Dynamics:** The battery is discharged at rated power for a fixed timestep. The energy removed from the battery is evaluated as:

$$E_{\text{removed}} = \frac{P_{\text{discharge}}}{\eta} \cdot \Delta t$$

The SOC reduction is verified accordingly.

– **Test Case 3 – SOC Limit Enforcement:** Charging and discharging commands are applied near the defined SOC_{max} and SOC_{min} limits. The model is verified to prevent overcharge and overdischarge by adjusting the actual power and clamping the SOC within its allowable range.

– **Test Case 4 – Power Constraints and Round-Trip Behavior:** Requested power values exceeding rated charge/discharge limits are evaluated to confirm internal clamping. A complete charge–discharge cycle is performed to verify the expected behavior.

5.2 System Integration Validation

Following component-level verification, a full system integration test was performed to validate the interaction between the Vessel, Charger, PV, and BESS models within the simulation environment.

Objective: Verify correct energy flow consistency, module interaction, and global power balance across a complete 24-hour simulation cycle.

Test Configuration:

– One electric vessel connected to a dedicated charger;

– Active PV generation with BESS;

– Fixed grid connection with contracted power limit.

Validation Criteria:

– Power balance consistency at each timestep:

$$P_{grid} + P_{PV} + P_{BESS} = P_{load}$$

– Compliance with all component constraints (power limits, SOC bounds, and capacity limits);

5.3 Port Electrification Studies

Following the unit validation, the framework is applied to a set of comprehensive studies focused on the Maritime-Tourism Pier of Funchal Port. As the primary pilot site for the *AHEAD* project, this location serves as a realistic testbed for evaluating the impact of increasing vessel electrification on grid stability and operational costs. Figure 14 illustrates the layout of the pier.

The study assumes a maximum theoretical fleet of 20 recreational vessels operating from this facility. To ensure a consistent baseline for comparison, the infrastructure is modeled with a 1-to-1 charger-to-vessel ratio, where each vessel is assigned a dedicated 22 kW AC charger ($\eta = 0.95$). The baseline grid connection is fixed at a contracted power limit of 80 kW.

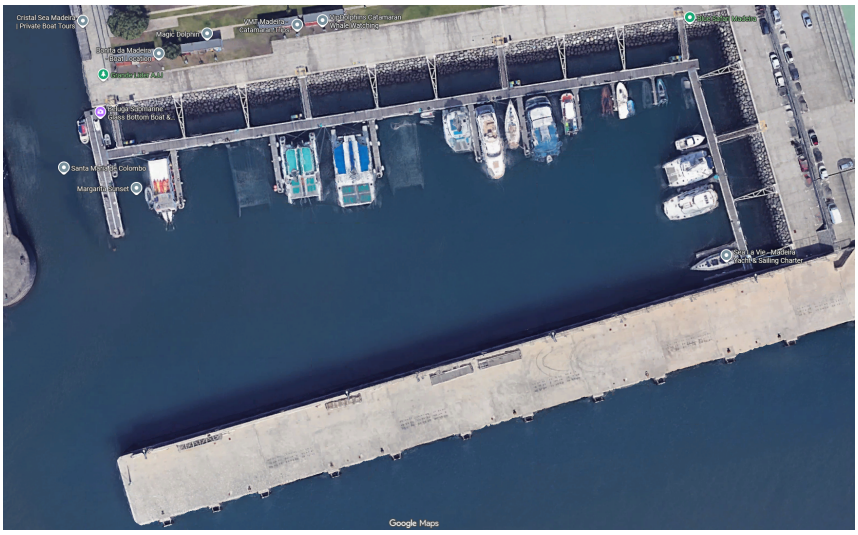

Figure. 14: Satellite view of the Maritime-Tourism Pier at Funchal Port.

To assess the scalability of the proposed solutions, each Use Case is simulated across three progressive Electrification Scenarios (25%, 50%, and 100%). These scenarios represent the gradual adoption of electric vessels (EVs) and the corresponding expansion of Distributed Energy Resources (DER), as detailed in Table 2. Each specific variation (Scenario A, B, or C) is simulated for

a duration of one day (24 hours) to capture a full diurnal cycle of solar generation and vessel activity.

Parameter	**Scenario A (25%)**	**Scenario B (50%)**	**Scenario C (100%)**
Electric Vessels	5	10	20
PV Capacity	15 kWp	30 kWp	60 kWp
BESS Capacity	25 kWh	50 kWh	100 kWh
Contracted Power	80 kW (Fixed)		

Table 2: Definition of Electrification Scenarios for Funchal Port.

5.3.1 Use Cases

The evaluation is structured around three core System Use Case (SUC) defined within the scope of the *AHEAD* project. These scenarios are designed to represent a spectrum of operational complexities, ranging from unmanaged baseline operations to complex management systems involving distributed resources.

The first scenario, **S.U.C. 1: Uncoordinated Charging**, establishes a baseline environment where no energy management strategies are applied. In this setup, vessels initiate charging immediately upon arrival at a maximum power of 22 kW and continue until the battery is fully charged. The primary purpose of this scenario is to highlight the raw impact on the grid resulting from uncoordinated charging operations.

The second scenario, **S.U.C. 2 (Part 1): Smart Charging (No DER)**, introduces smart charging logic but excludes local generation assets. The optimization strategy focuses on reducing peak power demand to strictly adhere to the 80 kW grid limit.

Finally, **S.U.C. 2 (Part 2): Smart Charging (With DER)** extends the previous smart charging logic by integrating the scalable PV and BESS assets defined in Table 2. In this scenario, the control strategy expands to include maximizing self-consumption and self-sufficiency while maintaining overall grid stability.

5.3.2 Key Performance Indicators

To quantitatively evaluate these scenarios, a set of KPIs was established. These metrics track the economic, operational, and technical efficiency of the proposed solutions across the different phases of electrification.

5.3.2.1 Total Cost of Operation

This indicator represents the absolute operational cost of the port microgrid over the simulation horizon T. The Total Cost of Operation (TCO) is calculated by summing the cost of energy drawn from the grid at each time step t, as shown in Equation 27:

$$KPI_{TCO} = \sum_{t=1}^{T} (P_{grid}(t) \cdot C_{grid}(t) \cdot \Delta t) \tag{27}$$

where $P_{grid}(t)$ is the power drawn from the grid at time t, $C_{grid}(t)$ is the electricity tariff at that moment, and Δt is the time interval duration.

5.3.2.2 Reduction in Cost of Operation

This metric quantifies the relative cost savings of the optimized scenarios compared to the unmanaged baseline. It is defined as the percentage difference between the baseline cost (KPI_{TCO}^{base}) and the optimized scenario cost (KPI_{TCO}^{opt}):

$$KPI_{\Delta Cost} = \frac{KPI_{TCO}^{base} - KPI_{TCO}^{opt}}{KPI_{TCO}^{base}} \times 100[\%] \tag{28}$$

5.3.2.3 Peak Power Demand Reduction

This indicator tracks the percentage reduction in peak grid power demand. It is calculated by comparing the maximum peak of the baseline (P_{max}^{base}) against the optimized scenario (P_{max}^{opt}):

$$KPI_{\Delta Peak} = \frac{P_{max}^{base} - P_{max}^{opt}}{P_{max}^{base}} \times 100[\%] \tag{29}$$

5.3.2.4 Self-Consumption Rate (SCR)

The Self-Consumption Rate (SCR) evaluates the efficiency of the renewable energy usage; it is defined as the ratio of the locally generated PV energy that is directly consumed by the port loads relative to the total PV energy generated. A higher SCR indicates less energy injection into the grid:

$$KPI_{SCR} = \frac{\sum_{t=1}^{T} \min\left(P_{load}(t), P_{PV}(t)\right) \cdot \Delta t}{\sum_{t=1}^{T} P_{PV}(t) \cdot \Delta t} \times 100[\%] \tag{30}$$

where $P_{load}(t)$ is the total power demand and $P_{PV}(t)$ is the available photovoltaic power generation.

5.3.2.5 Self-Sufficiency Rate (SSR)

The Self-Sufficiency Rate (SSR) measures the degree of independence from the external grid; it represents the share of the total port energy demand that is covered by locally generated renewable energy. Unlike SCR, the denominator here is the total load consumption:

$$KPI_{SSR} = \frac{\sum_{t=1}^{T} \min\left(P_{load}(t), P_{PV}(t)\right) \cdot \Delta t}{\sum_{t=1}^{T} P_{load}(t) \cdot \Delta t} \times 100[\%] \tag{31}$$

5.3.2.6 Port Reliability

Reliability is defined as the percentage of vessel trips that are able to depart on time with the required battery SOC. It is calculated by comparing the number of on-time departures (N_{ontime}) to the total number of scheduled trips (N_{total}):

$$KPI_{Reliability} = \frac{N_{ontime}}{N_{total}} \times 100[\%] \tag{32}$$

6 Results and Discussion

This chapter presents the results obtained from the *PyPort Sim* simulation environment. The analysis is divided into two primary sections: first, the validation of the individual software components; second, the evaluation of the port electrification studies, analyzing the operational, economic, and technical impacts of the proposed use cases, thereby addressing the research questions and objectives outlined in Chapter 1.

6.1 Unit Test Outcomes

Before conducting the full-scale port scenarios, the core asset models were subjected to the unit tests defined in Section 5.1.

6.1.1 Vessel Model

The reference configuration subject to testing is $P_{motor} = 500$ kW and $v_{range} = 10$ knots, therefore, the hydrodynamic coefficient is analytically defined as:

$$k = \frac{P_{motor}}{v_{range}^3} = \frac{500}{10^3} = 0.5$$

The model returned $k = 0.5$, matching the analytical value without deviation.

The cubic scaling relationship $P = kv^3$ was evaluated at multiple speeds. The analytical and computed values are shown in Table 3.

Speed (knots)	Analytical Power (kW)	Model Result (kW)
5.0	62.5	62.5
10.0	500.0	500.0
15.0	1687.5	1687.5

Table 3: Verification of Cubic Propeller Law

Figure 15 illustrates the cubic relationship between vessel speed and propulsion power. The reference operating point (10 knots, 500 kW) lies exactly on the computed curve.

Constructor validation tests confirmed strict enforcement of physical constraints. Specifically, initializations with non-positive motor power values, such as 0 or -100 kW, non-positive battery capacities, and SOC values outside the valid interval $[0, 1]$, such as -0.1 or 1.1, correctly raised `ValueError` exceptions.

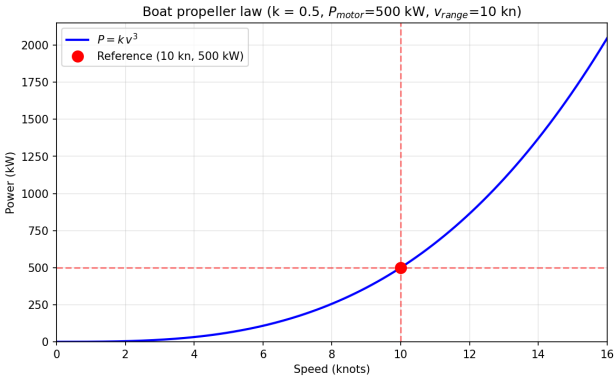

Figure. 15: Verification of the cubic propeller law implementation.

Furthermore, the internal state setter was verified to strictly accept only the predefined enumerated states: *IDLE*, *CHARGING*, and *SAILING*. Attempts to assign invalid data types or unrecognized states, such as arbitrary strings or integers, correctly triggered exceptions, ensuring robust state management during simulations.

6.1.2 Charger Model

The charger was configured with a rated maximum power $P_{max} = 22$ kW and efficiency $\eta_{evse} = 0.95$. Constructor validation tests confirmed that non-positive rated power values and efficiency values outside the interval $[0, 1]$ correctly raised `ValueError` exceptions. Initial power values outside the interval $[0, P_{max}]$ were also rejected.

Power clamping behavior was validated by applying requested charging powers exceeding the rated limit. Assigned power was limited according to $P_{assigned} = \min(P_{requested}, P_{max})$. The resulting effective charging power delivered was computed as $P_{eff} = P_{assigned} \cdot \eta_{evse}$. For instance, a valid request of 10.0 kW resulted in an assigned power of 10.0 kW and an effective delivery of 9.50 kW. Conversely, requests exceeding the 22.0 kW limit, such as 30.0 kW or 50.0 kW, were strictly clamped, resulting in a constant assigned power of 22.0 kW and a maximum effective delivery of 20.90 kW.

Figure 16 illustrates the relationship between requested, assigned, and effective charging power. For requests above 22 kW, the assigned power remains constant at the rated limit, while effective power reflects the applied efficiency factor.

The internal state setter was verified to strictly accept only the enumerated states *IDLE* and *CHARGING*. Attempts to assign non-enumerated values correctly triggered exceptions. Addition-

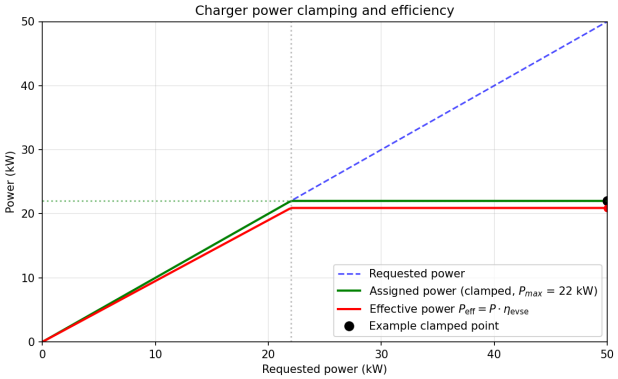

Figure. 16: Charger power clamping and efficiency behavior.

ally, transitions to the *IDLE* state automatically reset the output power to zero and cleared any connected vessel reference.

6.1.3 PV Model

The PV model was configured for the geographical coordinates of Funchal (32.65°N, 16.91°W) with a rated capacity of 22 kW, tilt angle of 9°, and south-facing orientation.

Night condition verification confirmed that for timestamps where the apparent solar elevation satisfies $\alpha \leq 0$, the model returns zero power output. Multiple night-time hours (00:00–05:00 and 22:00–23:00 UTC) were evaluated, and production was consistently equal to 0 kW.

A clear-sky summer solstice day (21 June 2025) was simulated to evaluate the diurnal production profile. The resulting power curve exhibits a bell-shaped behavior, with production increasing after sunrise, peaking near solar noon, and decreasing symmetrically toward sunset. The peak production reached 17.4 kW at approximately 12.5 h UTC, remaining below the rated capacity.

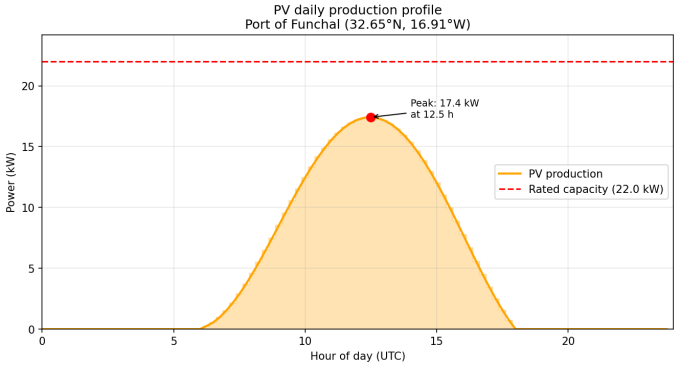

Figure. 17: Daily PV production profile under clear-sky conditions at Funchal.

Capacity constraint validation confirmed that instantaneous production never exceeded the rated capacity of 22 kW, even under high irradiance inputs (GHI = 1000 W/m^2).

6.1.4 BESS Model

The BESS model was configured with a capacity of 100 kWh, maximum charge and discharge power of ±50 kW, round-trip efficiency $\eta = 0.90$, and SOC limits defined within the interval 10 % - 90 %.

Charging dynamics were validated by applying rated charging power for a fixed duration and comparing the SOC variation against the analytical expectation $E_{stored} = P_{charge} \cdot \eta \cdot \Delta t$. For a one-hour charging interval at 50 kW, the resulting SOC increase matched the theoretical energy balance. In addition, discharging dynamics were verified using $E_{removed} = \frac{P_{discharge}}{\eta} \cdot \Delta t$. For a one-hour discharge at rated power, the SOC reduction corresponded exactly to the analytical prediction.

Figure 18 illustrates a representative charge–idle–discharge sequence. During charging, SOC increases linearly until reaching operational limits; during discharging, SOC decreases accordingly. Power remains clamped within ±50 kW and SOC remains strictly within the defined bounds.

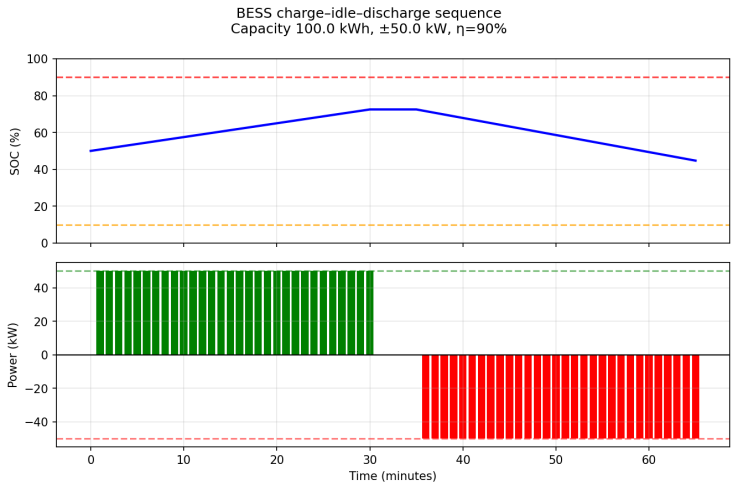

Figure. 18: BESS charge–idle–discharge sequence and SOC evolution.

A complete charge–discharge cycle was performed to verify round-trip behavior. The final SOC after the cycle was lower than the initial SOC, consistent with the imposed efficiency losses and matching the expectation of energy dissipation.

6.2 Integration Test Results

A full 24-hour batch simulation was executed to validate system-level consistency between the Vessel, Charger, PV, BESS, and grid models. The scenario included one electric vessel connected to a dedicated charger, active PV generation, a BESS unit, and a fixed grid connection with a contracted power limit of 80 kW.

Grid constraint validation confirmed that the maximum import power never exceeded the contracted limit of 80 kW. The highest observed import remained strictly within the allowed bound.

SOC limits were validated for both the vessel and the BESS. The BESS SOC remained within the defined interval of 10–90%, while vessel SOC remained within physical bounds of 0–100% throughout the simulation. Additionally, BESS charge and discharge power remained within its rated limits of ±30 kW.

Figure 19 presents the system-level power flows and SOC evolution over the 24-hour period. During the morning hours, PV production increases progressively, exceeding the instantaneous load. This surplus energy is absorbed by the BESS, as indicated by negative P_{BESS} values (charging mode) while P_{grid} remains close to zero. The BESS SOC correspondingly increases until reaching its upper operational limit.

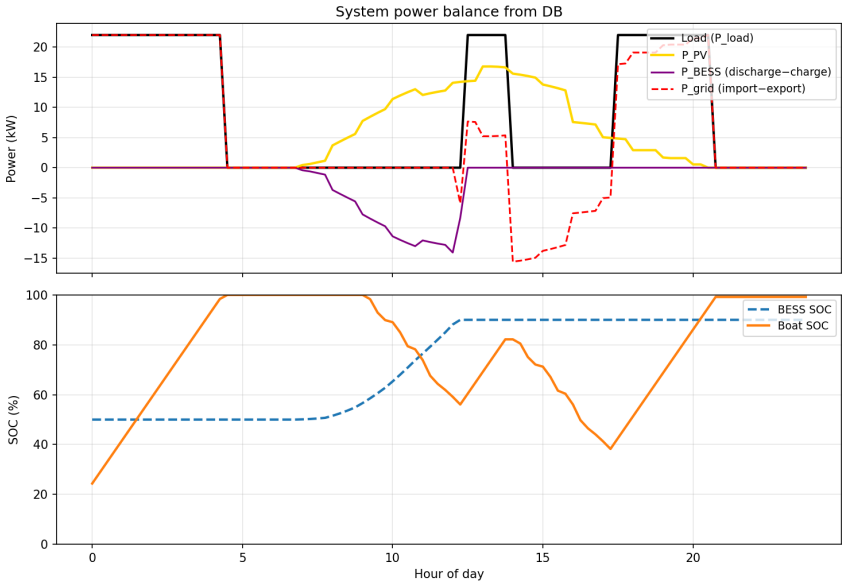

Figure. 19: System-level power balance and SOC evolution over a 24-hour simulation.

By following the boat SOC trajectory in the lower subplot, two distinct discharge events are observable, corresponding to two separate trips during the simulated day. Each reduction in SOC is followed by a recovery phase once the vessel reconnects to the charger.

Around midday, when vessel charging demand rises, PV production contributes directly to the load while the BESS transitions to discharge mode, supplying additional power and reducing grid import.

During periods of low or zero PV production, the system relies on grid import to satisfy load demand, as expected. Throughout the entire simulation horizon, SOC limits and power constraints remain respected, and the energy balance condition is preserved. These integration results directly answer the primary research question, confirming that the dynamic operations of the port can be reliably simulated, effectively establishing the framework as a practical precursor for a future Digital Twin.

6.3 Port Electrification Analysis

This section presents the results of the use-case simulations, the scenarios utilized the `SeaBreeze` vessel class, configured as a representative medium-sized commercial recreational vessel with a 100 kWh battery pack (see Table 4). In order to ensure comparability across scenarios and isolate the impact of fleet size, optimization strategy, and DER integration, all vessels were assumed to follow identical operational profiles. Specifically, each vessel performed the same predefined route with identical trip duration, departure times, and energy demand.

Parameter	**Value**
Battery Capacity	100 kWh
Motor Power	100 kW
Cruising Speed	16.0 knots
Initial SOC	0.50 (50%)

Table 4: Configuration of the `SeaBreeze` Vessel Class

6.3.1 5 Vessel Scenarios

The five vessel scenario represents a low demand configuration in which infrastructure constraints are not yet binding. Figure 20 presents the total daily energy contribution by source for the three evaluated configurations.

In the absence of optimization and DER, total energy demand is entirely supplied by grid import. When optimization is introduced, total grid energy decreases significantly, indicating im-

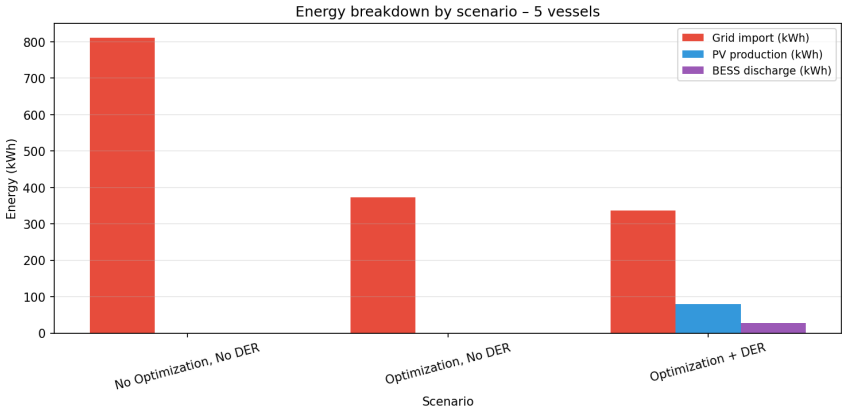

Figure. 20: Daily energy contribution by source (5 vessels).

proved temporal scheduling and reduced simultaneous charging peaks. With the addition of DER, a portion of the demand is supplied by PV production and BESS discharge, further reducing grid dependency.

Figure 21 illustrates the temporal load profiles relative to the contracted grid power of 80 kW.

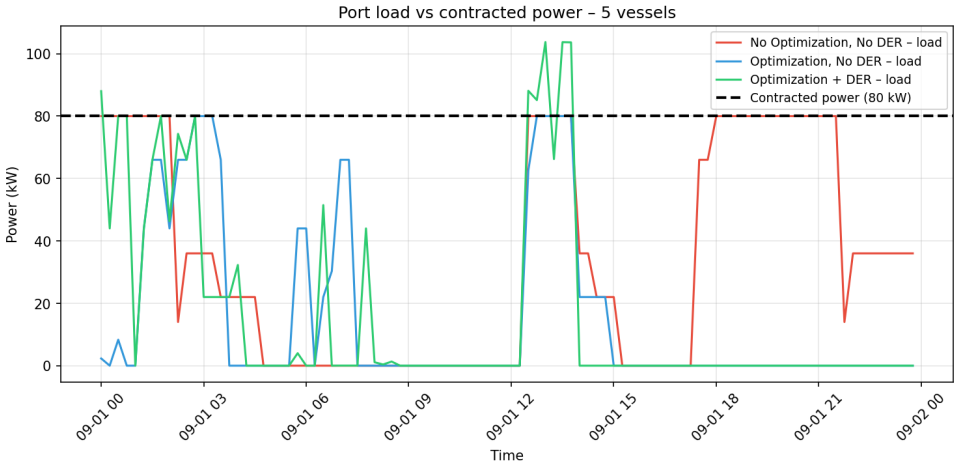

Figure. 21: Port load profiles compared to contracted grid power (5 vessels).

In the non-optimized case, load peaks approach the contracted limit during simultaneous charging events. Optimization redistributes charging demand more evenly throughout the day, reducing peak intensity and flattening the load curve. When DER is included, midday PV generation offsets part of the charging demand, and short-duration peaks above the contracted level are mitigated through BESS discharge.

Trip reliability results are presented in Figure 22.

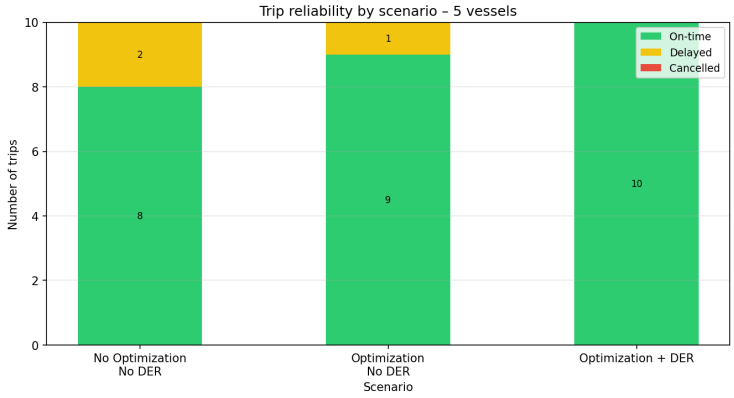

Figure. 22: Trip reliability outcomes (5 vessels).

Reliability remains at 100% across all configurations, with all scheduled trips completed successfully. However, optimization reduces minor scheduling delays observed in the baseline configuration. The integration of DER eliminates delays entirely, as local generation and storage provide additional flexibility during high-demand periods.

Overall, the five-vessel scenario demonstrates that optimization significantly reduces grid energy consumption without compromising reliability. DER integration further enhances energy autonomy and improves local resource utilization, although infrastructure capacity is not yet a limiting factor at this fleet size.

6.3.2 10 Vessel Scenarios

The ten vessel scenario represents a moderate demand configuration in which charging simultaneity increases and infrastructure constraints begin to influence operational performance. Figure 23 presents the total daily energy contribution by source for the three evaluated configurations.

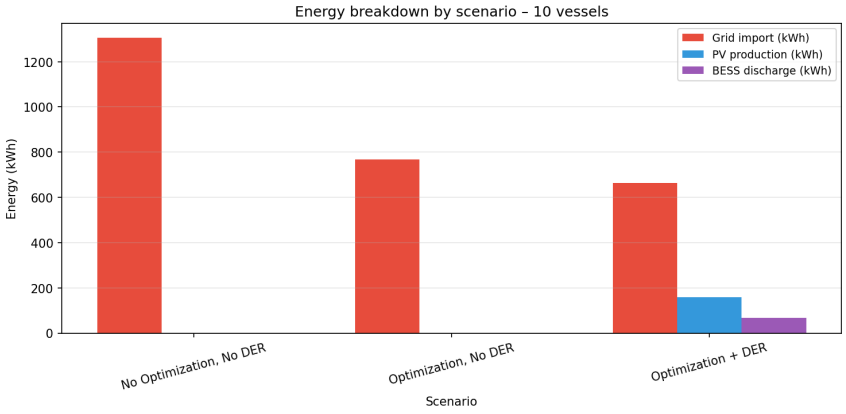

Figure. 23: Daily energy contribution by source (10 vessels).

In the absence of optimization and DER, total energy demand is fully supplied by grid import, resulting in the highest daily grid consumption among the three configurations. The introduction of smart charging significantly reduces grid energy usage by redistributing charging activity and limiting simultaneous high-power events. When DER is integrated, a substantial portion of the demand is supplied locally through PV production and BESS discharge, further decreasing grid dependency and improving local energy utilization.

Figure 24 illustrates the temporal load profiles relative to the contracted grid power of 80 kW.

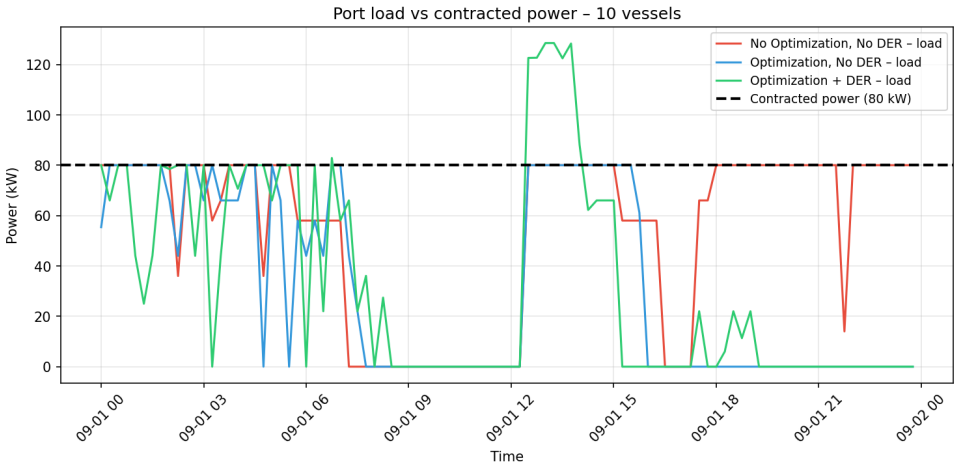

Figure. 24: Port load profiles compared to contracted grid power (10 vessels).

In the non-optimized configuration, multiple time intervals reach the contracted power limit due to simultaneous vessel charging. Although the limit is not exceeded, the system operates persistently near its maximum capacity. Optimization smooths the load distribution, reducing peak intensity and flattening the charging profile. With DER integration, midday PV generation offsets part of the charging demand, and the BESS mitigates short-duration peaks, improving operational flexibility.

Trip reliability results are presented in Figure 25.

In the baseline case, several trips experience delays due to insufficient charging time under high simultaneity conditions. Smart charging reduces the number of delayed departures by prioritizing energy allocation more effectively. The integration of DER further improves reliability by providing additional local generation and storage support during peak demand periods.

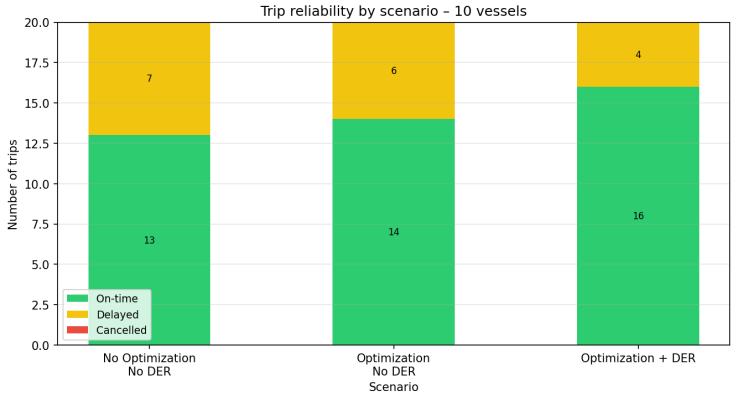

Figure. 25: Trip reliability outcomes (10 vessels).

Overall, the ten-vessel scenario highlights the increasing importance of coordinated charging strategies. While infrastructure limits are not yet critically binding, optimization and DER integration demonstrably improve both energy efficiency and operational reliability.

6.3.3 20 Vessel Scenarios

The twenty vessel scenario represents a high demand configuration in which infrastructure constraints become binding and system limitations begin to directly affect operational performance. Figure 26 presents the total daily energy contribution by source for the three evaluated configurations.

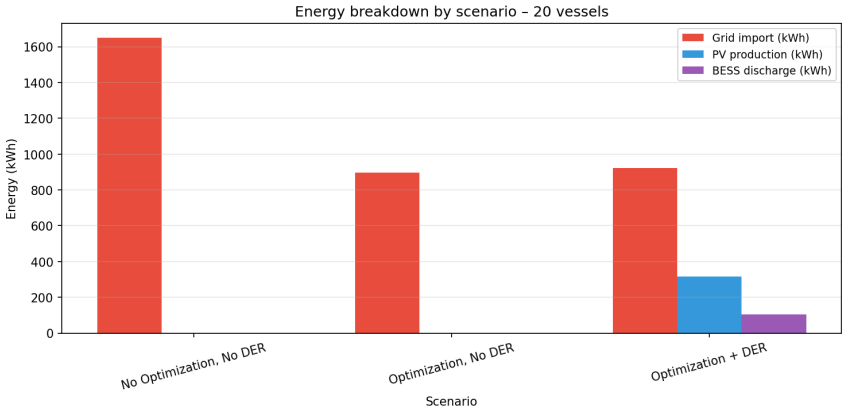

Figure. 26: Daily energy contribution by source (20 vessels).

In the absence of optimization and DER, total demand is supplied entirely by grid import, resulting in the highest daily grid energy consumption among all fleet sizes. The introduction of optimization significantly reduces grid energy requirements, indicating improved temporal co-

ordination of charging activities. However, at this fleet size, optimization alone is insufficient to eliminate infrastructure stress.

When DER is integrated, PV production and BESS discharge contribute substantially to meeting demand. Although total grid import remains considerable due to the high aggregate load, local generation and storage meaningfully offset peak-period consumption and improve overall energy autonomy.

Figure 27 illustrates the temporal load profiles relative to the contracted grid power of 80 kW.

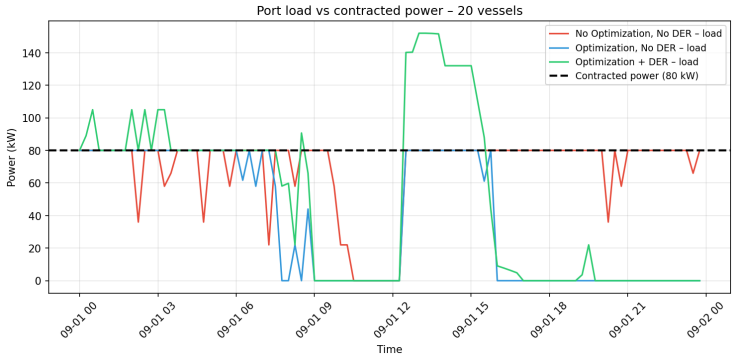

Figure. 27: Port load profiles compared to contracted grid power (20 vessels).

In both the non-optimized and optimized scenarios without DER, the contracted power limit is reached frequently during simultaneous charging events. The load profile becomes highly constrained, indicating that the grid connection is operating at its maximum allowable capacity for extended periods.

With the inclusion of DER, midday PV generation combined with BESS discharge mitigates part of the overload during peak demand intervals. Although instantaneous total load may exceed the contracted limit internally, the grid import component remains regulated through local generation support.

Trip reliability results are presented in Figure 28.

At this fleet size, reliability is no longer preserved across all configurations. Optimization increases the number of on-time trips from 17 to 24, corresponding to an improvement of approximately 41%. This performance gain is achieved at the expense of a redistribution of service outcomes, including one additional cancelled trip occurring in the evening period. This trade-off arises from the structure of the optimization objective function, which assigns a higher reward to on-time

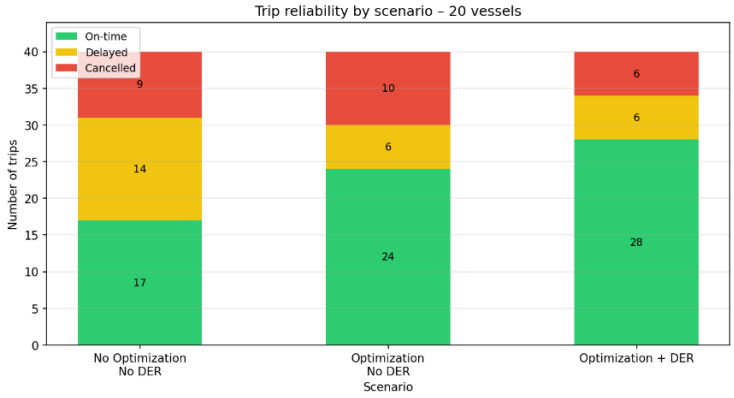

Figure. 28: Trip reliability outcomes (20 vessels).

departures than to delay minimization. Consequently, the optimizer prioritizes allocating available charging capacity to maximize the number of punctual trips, even if this results in isolated cancellations under severe infrastructure constraints.

The integration of DER produces the most significant reliability improvement. On-time trips increase considerably, while both delayed and canceled trips are reduced. The presence of local generation and storage provides additional flexibility during high-demand periods, directly improving service continuity.

Overall, the twenty vessel scenario demonstrates the transition from an energy-efficiency problem to a capacity-constrained operational problem. At higher fleet penetration levels, optimization alone is insufficient to guarantee service reliability, and DER integration becomes a critical enabler of operational resilience.

6.3.4 Performance Trends Across Scenarios

Table 5 consolidates the Key Performance Indicators across all fleet sizes and operational configurations, enabling a structured comparison of reliability, economic performance, grid stress, and renewable integration as electrification levels increase.

Vessels	Scenario	Reliability (%)	Cost (€)	€/Trip	Self-Cons. (%)	Self-Suff. (%)
5	No Optimization, No DER	100.0	142.38	14.24	-	-
5	Optimization, No DER	100.0	62.64	6.26	-	-
5	Optimization + DER	100.0	53.85	5.39	55.6	11.5
10	No Optimization, No DER	100.0	219.71	10.99	-	-
10	Optimization, No DER	100.0	127.78	6.39	-	-
10	Optimization + DER	100.0	102.99	5.15	83.0	16.5
20	No Optimization, No DER	77.5	296.68	9.57	-	-
20	Optimization, No DER	75.0	145.48	4.85	-	-
20	Optimization + DER	85.0	148.02	4.35	84.5	22.4

Table 5: Key Performance Indicators for Port Electrification Scenarios.

6.3.4.1 Reliability Evolution

For the 5- and 10-vessel scenarios, trip reliability remains at 100% across all configurations. This indicates that, at low and moderate electrification levels, the contracted grid capacity of 80 kW is sufficient to meet charging demand without compromising operational continuity.

A structural transition occurs in the 20-vessel scenario. In the absence of DER, reliability decreases to 77.5% in the baseline configuration and 75.0% under smart charging. Although optimization significantly reduces cost, it does not guarantee improved reliability under high simultaneity conditions. This reflects the objective function prioritization, which maximizes punctual departures rather than minimizing cancellations. Under binding infrastructure constraints, charging allocation becomes a limited-resource optimization problem in which not all service requirements can be satisfied simultaneously.

The integration of DER increases reliability to 85.0%, demonstrating that local generation and storage provide additional flexibility during peak demand periods. At high electrification levels, DER therefore transitions from an efficiency-enhancing component to a reliability-enabling infrastructure element.

6.3.4.2 Operational Cost and Cost per Trip

Across all fleet sizes, smart charging produces substantial cost reductions compared to the unmanaged baseline. At 5 vessels, total daily cost decreases by approximately 56%. At 10 vessels, cost decreases by approximately 42%, and at 20 vessels by approximately 51%. These results confirm that temporal coordination of charging demand yields consistent economic benefits.

When DER is integrated, additional cost reductions are observed in the 5- and 10-vessel scenarios. However, at 20 vessels, the DER-integrated configuration presents a slightly higher total

cost than the optimized-only case. This marginal difference reflects the trade-off between strict economic minimization and improved service reliability. While DER enhances operational continuity, it does not always guarantee the lowest short-term expenditure under heavily constrained conditions.

6.3.4.3 Peak Demand and Grid Utilization

The maximum grid import remains capped at 80 kW across all configurations, confirming strict enforcement of the contracted power limit. However, the interpretation of this value evolves with fleet size.

At 5 vessels, the peak is approached intermittently. At 10 vessels, the system operates frequently near the constraint. At 20 vessels, the grid limit becomes persistently binding, indicating that infrastructure capacity is structurally saturated for extended periods.

6.3.4.4 Renewable Integration Indicators

Self-Consumption Rate (SCR) and Self-Sufficiency Rate (SSR) increase with fleet size. SCR rises from 55.6% to 83.0% and 84.5% as electrification progresses from 5 to 20 vessels. Similarly, SSR increases from 11.5% to 22.4%. These results indicate that higher aggregate demand improves local PV utilization and increases the share of load supplied by renewable energy.

Overall, the results confirm that smart charging delivers consistent economic benefits across all penetration levels, while DER integration becomes strategically necessary once grid capacity saturation occurs. Ultimately, these findings address the secondary research question by quantifying the tangible impacts of optimization-based energy management on port reliability and grid utilization, fulfilling the overarching objectives of this thesis.

7 Conclusion

The electrification of recreational ports introduces tightly coupled operational and energy-management challenges that cannot be addressed through isolated component sizing alone. This thesis developed a structured simulation and optimization framework to support planning decisions under constrained infrastructure, variable demand, and limited historical data. The objective was to design a digital-twin–oriented environment capable of representing vessels, charging infrastructure, distributed energy resources, and grid interaction within a unified computational architecture, while remaining sufficiently modular to evolve toward real-world deployment.

7.1 Summary of Contributions

This work introduced PyPort Sim, a modular platform for modeling, simulating, and optimizing electrified recreational port operations. The architecture separates computation, state persistence, prediction, optimization, and visualization, enabling reproducibility of experiments and progressive system expansion. The design supports structured scenario studies and provides a foundation for future digital twin integration.

An integrated modeling framework was developed to capture the interaction between maritime demand and port energy infrastructure. Vessel propulsion demand was represented through a cubic speed–power relationship with explicit battery state tracking. Trip scheduling logic ensured feasibility through state-of-charge validation and postponement rules. EVSE behavior included power limits and efficiency modeling. Photovoltaic generation was computed from meteorological inputs, and a battery energy storage system model incorporated charge and discharge efficiencies with dynamic state evolution. All components were coordinated within a discrete-time simulation engine that preserved energy balance and operational causality.

A prediction layer was implemented to estimate future conditions for operational planning. Day-ahead PV production predictions—derived from weather forecasts—and pre-calculated vessel energy demand profiles were generated and stored as structured objects, enabling decoupled experimentation between prediction and scheduling. This structure provides a foundation for the future integration of more advanced, real-time forecasting techniques.

A Mixed-Integer Linear Programming formulation was implemented for day-ahead scheduling of grid import, charger allocation, and BESS dispatch. The optimization respected contracted grid

limits, vessel availability constraints, and storage dynamics. The objective function balanced energy cost with service performance using structured reward and penalty terms, including incentives for on-time departures and penalties for missed trips.

7.2 Challenges and Insights

Data scarcity represented a primary modeling constraint. Recreational boating datasets are often incomplete, irregular, or insufficiently annotated for direct energy modeling. Assumptions were therefore required to reconstruct trip behavior and operational schedules. The simulator was designed to remain transparent regarding these assumptions, enabling scenario exploration rather than strict historical replication.

Balancing model fidelity with computational tractability was a central design consideration. Highly detailed hydrodynamic or electrochemical models were avoided in favor of physically consistent representations that preserve energy conservation, enforce operational feasibility, and remain computationally efficient.

Simulation results highlighted that simultaneity, rather than total daily energy consumption, drives infrastructure stress. Charging overlap during limited berthing windows produces short-duration power peaks that define grid sizing requirements. Coordinated charging reduces peak demand without altering aggregate energy consumption, demonstrating the operational value of scheduling even at moderate fleet sizes.

Optimization consistently reduced operational costs across all evaluated scenarios. However, increasing fleet penetration revealed a transition from an efficiency-dominated regime to a capacity-constrained regime. Under high electrification levels and fixed contracted power, reliability declines emerged when infrastructure saturation occurred. Optimization alone could not fully restore service quality when structural capacity limits were binding.

Distributed energy resources shifted from cost-enhancing assets at low penetration levels to reliability-supporting assets at high penetration levels. Photovoltaic generation and storage mitigated peak demand periods and improved operational continuity under stressed conditions. Renewable utilization increased with demand intensity, indicating improved alignment between generation and consumption as system scale expanded.

Objective-function design proved critical in shaping scheduling outcomes. The trade-off between delayed and missed trips under constrained capacity demonstrated that optimization results depend on how service priorities are encoded. Operational policy choices therefore directly influence energy-management behavior when resources are insufficient to satisfy all demand simultaneously.

7.3 Limitations

While this thesis successfully demonstrated the value of the proposed simulation framework, several limitations must be acknowledged. First, as noted in the modeling challenges, the scarcity of real-world recreational boating datasets required the use of synthetic or assumed operational profiles. The absence of real operational data currently limits the absolute realism of the simulation outcomes, meaning the results are more indicative of system behavior under assumed conditions rather than exact reflections of a specific port's daily reality.

Second, the framework is constrained by the specific prediction and optimization methods implemented in this iteration. The energy management module relies primarily on deterministic, day-ahead scheduling, which does not fully capture the intra-day stochastic variability of maritime demand or real-time grid adjustments.

Finally, although the architecture was designed as a precursor to a Digital Twin, the current platform remains an offline simulation environment. It does not yet feature the live data ingestion, real-time monitoring, or closed-loop control mechanisms required to function as a fully operational Digital Twin capable of autonomous real-time decision-making.

7.4 Future Work

Future extensions should incorporate heterogeneous vessel categories with differentiated propulsion characteristics, battery capacities, and charging capabilities. Behavioral demand modeling incorporating seasonality, weather sensitivity, and user diversity would enhance realism and improve stress-testing of infrastructure strategies.

The implementation of true forecasting and optimization under uncertainty represent a natural progression. Robust or stochastic optimization frameworks and receding-horizon control strategies would better capture variability in PV production and maritime demand. Performance evaluation based on operational regret rather than prediction error alone would align predictive modeling with decision quality.

Integration of bidirectional energy concepts, including boat-to-grid operation and ancillary service participation, would extend the framework toward active energy ecosystems. Such developments require coordinated modeling of regulatory, technical, and economic dimensions.

Deployment as a decision-support tool for port operators is a key long-term goal of this work. Connecting the platform to real port data, such as energy meters, charger monitoring systems, and daily vessel schedules, would directly address current limitations by allowing the model to be calibrated and validated using actual operating conditions. Over time, the system could evolve from a scenario-based simulation tool into a live digital twin that reflects real port activity and supports day-to-day operational decisions. This progression would provide port managers with a reliable and intuitive tool to plan infrastructure investments, manage charging operations, and support the transition toward electrified maritime-tourism activities.

References

[1] C. S. Chin, C. Zhang, and Z. Gao, "Deploying battery technology for marine vessel electrification," *IEEE Potentials*, vol. 40, no. 6, pp. 24–33, 2021.

[2] N. N. Abu Bakar, N. Bazmohammadi, J. C. Vasquez, and J. M. Guerrero, "Electrification of onshore power systems in maritime transportation towards decarbonization of ports: A review of the cold ironing technology," *Renewable and Sustainable Energy Reviews*, vol. 178, p. 113243, 2023. [Online]. Available: https://www.sciencedirect.com/science/article/pii/S1364032123000990

[3] M. Sadiq, S. W. Ali, Y. Terriche, M. U. Mutarraf, M. A. Hassan, K. Hamid, Z. Ali, J. Y. Sze, C.-L. Su, and J. M. Guerrero, "Future greener seaports: A review of new infrastructure, challenges, and energy efficiency measures," *IEEE Access*, vol. 9, pp. 75 568–75 587, 2021.

[4] V. Selén, "Addressing ship emissions at berth: Onshore power supply where it makes sense," *IEEE Electrification Magazine*, vol. 11, no. 1, pp. 25–32, 2023.

[5] D. Filimon, "Status of the marinas' development in the southern region of the romanian sea coast: Implications for sustainable recreational transport in the black sea," *Sustainability*, vol. 15, no. 10, 2023. [Online]. Available: https://www.mdpi.com/2071-1050/15/10/7979

[6] A. Ibabe, Y. Borrell, S. Knobelspiess, and E. Dopico, "Perspectives on the marine environment and biodiversity in recreational ports: The marina of gijon as a case study," *Marine Pollution Bulletin*, vol. 160, p. 111645, 2020. [Online]. Available: https://www.sciencedirect.com/science/article/pii/S0025326X20307633

[7] B. D. Allen, "Digital twins and living models at nasa," in *Digital Twin Summit*, 2021.

[8] B. R. Barricelli, E. Casiraghi, and D. Fogli, "A survey on digital twin: Definitions, characteristics, applications, and design implications," *IEEE Access*, vol. 7, pp. 167 653–167 671, 2019.

[9] A. Fuller, Z. Fan, C. Day, and C. Barlow, "Digital twin: Enabling technologies, challenges and open research," *IEEE Access*, vol. 8, pp. 108 952–108 971, 2020.

[10] IBM. (2024) What is a digital twin? Accessed: 2024-05-22. [Online]. Available: https://www.ibm.com/think/topics/digital-twin

[11] L. Zhang, L. Zhou, and B. K. Horn, "Building a right digital twin with model engineering," *Journal of Manufacturing Systems*, vol. 59, pp. 151–164, 2021.

[12] T. L. Leirmo, "Digital twins for industry 5.0: Unlocking the human potential," *Procedia CIRP*, vol. 130, pp. 761–766, 2024.

[13] F. Zhou, K. Yu, W. Xie, J. Lyu, Z. Zheng, and S. Zhou, "Digital twin-enabled smart maritime logistics management in the context of industry 5.0," *IEEE Access*, vol. 12, pp. 10 920–10 931, 2024.

[14] Matterport. (2024) What is a digital twin? definition, types, and uses. Accessed: 2024-05-22. [Online]. Available: https://matterport.com/learn/digital-twin/overview

[15] R. Mao, Y. Li, and H. Zhang, "Digital twin-based research in the maritime industry: A brief survey," in *IECON 2023- 49th Annual Conference of the IEEE Industrial Electronics Society*, 2023, pp. 1–6.

[16] R. Klar, A. Fredriksson, and V. Angelakis, "Digital twins for ports: Derived from smart city and supply chain twinning experience," *IEEE Access*, vol. 11, pp. 71 777–71 799, 2023.

[17] M. Zhu, C. Calderon, A. Ford, C. Robson, and J. Jin, "Digital twin for resilience and sustainability assessment of port facility," *Sustainable and Resilient Infrastructure*, vol. 0, no. 0, pp. 1–34, 2024. [Online]. Available: https://doi.org/10.1080/23789689.2025.2526928

[18] D. Jesus, T. Oliveira, M. Perdigão, and A. Mendes, "Plugging into onshore power supply system innovation: A review from standards and patents to port deployment," *Energies*, vol. 18, no. 20, p. 5449, 2025.

[19] L. Fernández. (2025, Nov.) Breakdown of co2 emissions in the transportation sector worldwide 2024, by sub-sector. Statista. Accessed: 2026-01-06. [Online]. Available: https://www.statista.com/statistics/1185535/transport-carbon-dioxide-emissions-breakdown/

[20] T. T. N. Minh, H.-T. H. Hoang, H. S. Nam, A. S. Alamoush, and P. A. Duong, "Revisiting port decarbonization for advancing a sustainable maritime industry: Insights from bibliometric review," *Sustainability*, vol. 17, no. 10, p. 4302, 2025.

[21] S. B. Issa-Zadeh and C. L. Garay-Rondero, "Decarbonizing seaport maritime traffic: Finding hope," *World*, vol. 6, no. 2, p. 47, 2025.

[22] M. Amaral, N. Amaro, and P. Arsénio, "Methodology for assessing power needs for onshore power supply in maritime ports," *Sustainability*, vol. 15, no. 24, p. 16670, 2023.

[23] D. V. Lyridis, J. M. Prousalidis, A.-M. Lekka, V. Georgiou, and L. Nakos, "Holistic energy transformation of ports: The proteus plan," *IEEE Electrification Magazine*, vol. 11, no. 1, pp. 8–17, 2023.

[24] N. N. A. Bakar, N. Bazmohammadi, J. C. Vasquez, and J. M. Guerrero, "Electrification of onshore power systems in maritime transportation towards decarbonization of ports: A review of the cold ironing technology," *Renewable and Sustainable Energy Reviews*, vol. 178, p. 113243, 2023.

[25] C. L. Vásquez, F. A. Borges, L. Marinho, J. C. Hernández, and T. Batista, "Onshore power supply in multi-terminal maritime ports," *Energies*, vol. 18, no. 10, p. 2489, 2025.

[26] J. Qi, S. Wang, and C. Peng, "Shore power management for maritime transportation: Status and perspectives," *Maritime Transport Research*, vol. 1, p. 100004, 2020.

[27] T. Høven, "Standardization of utility connections in ports: Cold ironing of ships in ports," *IEEE Electrification Magazine*, vol. 11, no. 1, pp. 18–24, 2023.

[28] A. Paraskevas, M. Madas, V. Zeimpekis, and K. Fouskas, "Smart ports in industry 4.0: A systematic literature review," *Logistics*, vol. 8, no. 1, p. 28, 2024.

[29] H. N. Psaraftis and S. Lagouvardou, "Ship speed vs power or fuel consumption: Are laws of physics still valid? regression analysis pitfalls and misguided policy implications," *Cleaner Logistics and Supply Chain*, vol. 7, p. 100111, 2023.

[30] C.-o. Lim, B.-c. Park, J.-c. Lee, E. S. Kim, and S.-c. Shin, "Electric power consumption predictive modeling of an electric propulsion ship considering the marine environment," *International Journal of Naval Architecture and Ocean Engineering*, vol. 11, no. 2, pp. 765–781, 2019.

[31] B. J. Cipriano, R. J. Cruzate, S. Diokno, F. Samonte, L. J. de Luna, L. A. Tria, K. Vergel, P. Rodgers, C. M. Odulio, and E. Abaya, "Modeling and analysis of the voyage cycle for

ferryboat electrification," *Maritime Technology and Research*, vol. 5, no. 3, pp. 261 999–261 999, 2023.

[32] N. Costa, J. Ekholm, S. Rogerson, S. Janhäll, T. Besker, and T. Linders, "Standards of shore-side charging for battery-powered vessels: Technical report," RISE - Research Institutes of Sweden, Tech. Rep., 2022.

[33] W. Alfraidi, M. Shalaby, and F. Alaql, "Modeling ev charging station loads considering on-road wireless charging capabilities," *World Electric Vehicle Journal*, vol. 14, no. 11, p. 313, 2023.

[34] J. Kumar, A. A. Memon, L. Kumpulainen, K. Kauhaniemi, and O. Palizban, "Design and analysis of new harbour grid models to facilitate multiple scenarios of battery charging and onshore supply for modern vessels," *Energies*, vol. 12, no. 12, p. 2354, 2019.

[35] J. Ma and Y. Zhang, "Port microgrid capacity planning under tightening carbon constraints: A bi-level cost optimization framework," *Electronics*, vol. 14, no. 21, p. 4307, 2025.

[36] D. Pasculescu, S. Riurean, M. Ilieva-Obretenova, T. Lazar, A. M. Tatar, and N. D. Fita, "Intelligent modeling of pv–bess microgrids for enhanced stability, cyber–physical resilience and blackout prevention," *Energies*, vol. 19, no. 1, 2026. [Online]. Available: https://www.mdpi.com/1996-1073/19/1/148

[37] M. Rana, M. Romlie, M. Abdullah, M. Uddin, and M. Rahman, "Modeling of an isolated microgrid with hybrid pv-bess system for peak load shaving simulation," *International Journal of Advanced Technology and Engineering Exploration*, vol. 8, pp. 352–361, 02 2021.

[38] A. Zapata, "Power flow modeling and analysis of a green seaport power system," Master's thesis, California Polytechnic State University, 2024.

[39] T. Cao and Y. Xu, "An end-to-end approach for microgrid probabilistic forecasting and robust operation via decision-focused learning," *arXiv preprint arXiv:2512.12755*, 2025.

[40] D. Colarossi, V. D'Alessandro, L. Giammichele, M. Falone, and R. Ricci, "Development of a renewable energy forecasting strategy based on numerical weather prediction for the cold ironing system at the port of ancona, italy," *International Journal of Energy Production and Management. 2024. Vol. 9. Iss. 4*, vol. 9, no. 4, pp. 201–208, 2024.

[41] R. Tang, S. Ning, Z. Ren, X. Li, and Y. Zhang, "Novel load forecasting and optimal dispatching methods considering demand response for integrated port energy system," *Journal of Marine Science and Engineering*, vol. 13, no. 3, p. 421, 2025.

[42] A. Carrillo-Galvez, F. do Carmo, T. Soares, Z. Mourão, I. Ponomarev, J. Araújo, and E. Bandeira, "Electricity demand forecasting in green ports: Modelling and future research directions," *Transport Policy*, 2025.

[43] G. Kim, G. Lee, S. An, and J. Lee, "Forecasting future electric power consumption in busan new port using a deep learning model," *The Asian Journal of Shipping and Logistics*, vol. 39, no. 2, pp. 78–93, 2023.

[44] A. Alsafrani, H. I. Sherazi, O. Alrumayh, S. Habib, A. A. Alburidy, and M. Islam, "Photovoltaic power forecasting for sustainable grid integration: A hybrid deep learning approach," *IEEE Access*, vol. 13, pp. 216 013–216 025, 2025.

[45] A. Micallef, M. Apap, J. Licari, C. S. Staines, and Z. Xiao, "A comparative framework for evaluating machine learning models in forecasting electricity demand for port microgrids," *Energy and AI*, vol. 20, p. 100494, 2025.

[46] L. Hernandez, C. Baladron, J. M. Aguiar, B. Carro, A. J. Sanchez-Esguevillas, J. Lloret, and J. Massana, "A survey on electric power demand forecasting: future trends in smart grids, microgrids and smart buildings," *IEEE Communications Surveys & Tutorials*, vol. 16, no. 3, pp. 1460–1495, 2014.

[47] P. Song, H. Zhu, and Q. Yang, "Short-term high-volatility power load forecasting in smart port energy systems using featuregating-bilstm enhanced by dualattention mechanisms," *Energy Conversion and Management*, vol. 348, p. 120664, 2026.

[48] V. Álvarez, S. Mazuelas, and J. A. Lozano, "Probabilistic load forecasting based on adaptive online learning," *IEEE Transactions on Power Systems*, vol. 36, no. 4, pp. 3668–3680, 2021.

[49] Y. Yang, H. M. Hussain, J. Haakana, and P. Nardelli, "Assessing the technical and environmental impacts of energy management systems in smart ports," *arXiv preprint arXiv:2511.20043*, 2025.

[50] F. Binot, S. Meunier, V. Reinbold, M. Petit, S. Correcher, and K. Mamadou, "Optimization of the design of photovoltaic-based seaport microgrids considering techno-economic and environmental criteria," *Energy Reports*, vol. 11, pp. 5819–5830, 2024. [Online]. Available: https://www.sciencedirect.com/science/article/pii/S2352484724003305

[51] P. Ge, D. Tang, Y. Yuan, J. M. Guerrero, and E. Zio, "A hierarchical multi-objective co-optimization framework for sizing and energy management of coupled hydrogen-electricity energy storage systems at ports," *Applied Energy*, vol. 384, p. 125451, 2025. [Online]. Available: https://www.sciencedirect.com/science/article/pii/S0306261925001813

[52] C. Xiong, Y. Su, H. Wang, D. Zhang, and B. Xiong, "Optimal distributed energy scheduling for port microgrid system considering the coupling of renewable energy and demand," *Sustainable Energy, Grids and Networks*, vol. 39, p. 101506, 2024. [Online]. Available: https://www.sciencedirect.com/science/article/pii/S2352467724002352

[53] H. M. Ramos, J. S. Coelho, E. Bekci, T. X. Adrover, O. E. Coronado-Hernández, M. Perez-Sanchez, K. Koca, A. McNabola, and R. Espina-Valdés, "Optimization and machine learning in modeling approaches to hybrid energy balance to improve ports' efficiency," *Applied Sciences*, vol. 15, no. 9, p. 5211, 2025.

[54] Ç. Iris and J. S. L. Lam, "Optimal energy management and operations planning in seaports with smart grid while harnessing renewable energy under uncertainty," *Omega*, vol. 103, p. 102445, 2021.

[55] N. N. Abu Bakar, N. Bazmohammadi, J. C. Vasquez, and J. M. Guerrero, "Seaside port operation optimization and energy management system with integrated seaport microgrid and cold ironing," *Next Energy*, vol. 9, p. 100439, 2025. [Online]. Available: https://www.sciencedirect.com/science/article/pii/S2949821X25002029

[56] L. Maloberti and R. Zaccone, "An environmentally sustainable energy management strategy for marine hybrid propulsion," *Energy*, vol. 316, p. 134517, 2025.

[57] D. Jozwiak, J. R. Pillai, P. Ponnaganti, B. Bak-Jensen, and J. Jantzen, "Optimising energy flexibility of boats in pv-bess based marina energy systems," *Energies*, vol. 14, no. 12, p. 3397, 2021.

[58] M. Eneström and M. Dryagina, "Energy and revenue optimization of marinas with electric leisure boats by utilizing b2g: An optimization model for marinas located in gothenburg," Ph.D. dissertation, Uppsala University, 2025. [Online]. Available: https://urn.kb.se/resolve?urn=urn:nbn:se:uu:diva-563499

[59] P. M. Nadkarni, L. Marenco, R. Chen, E. Skoufos, G. Shepherd, and P. Miller, "Organization of heterogeneous scientific data using the eav/cr representation," *Journal of the American Medical Informatics Association*, vol. 6, no. 6, pp. 478–493, 11 1999. [Online]. Available: https://doi.org/10.1136/jamia.1999.0060478

[60] L. Larsson and R. E. Eliasson, *Principles of Yacht Design*, 4th ed. International Marine / McGraw-Hill, 2014.

[61] K. S. Ng, C.-S. Moo, Y.-P. Chen, and Y.-C. Hsieh, "Enhanced coulomb counting method for estimating state-of-charge and state-of-health of lithium-ion batteries," *Applied energy*, vol. 86, no. 9, pp. 1506–1511, 2009.

[62] S. Fang, Y. Wang, B. Gou, and Y. Xu, "Toward future green maritime transportation: An overview of seaport microgrids and all-electric ships," *IEEE Transactions on Vehicular Technology*, vol. 69, no. 1, pp. 207–219, 2019.

[63] GeeksforGeeks. (2023) Software engineering | sdlc v-model. Accessed: 2026-02-13. [Online]. Available: https://www.geeksforgeeks.org/software-engineering-sdlc-v-model/